First principles study of the ground and excited states of FeO, FeO^+, and FeO^-

Constantine N. Sakellaris, Evangelos Miliordos, and Aristides Mavridis[a)]
Department of Chemistry, Laboratory of Physical Chemistry, National and Kapodistrian University of Athens, Panepistimiopolis, Athens 157 71, Greece

(Received 31 March 2011; accepted 19 May 2011; published online 17 June 2011)

Through a variety of highly correlated methods combined with large basis sets we have studied the electronic structure of FeO, FeO^+, and FeO^-. In particular, we have constructed complete potential energy curves for 48, 24, and 4 states for the FeO, FeO^+, and FeO^- species, respectively, at the multireference level of theory. For all states examined we report energetics, common spectroscopic parameters, and dipole moments. Overall our results are in good agreement with experiment, but we have encountered as well interesting differences between experiment and theory deserving further investigation. © *2011 American Institute of Physics*. [doi:10.1063/1.3598529]

I. INTRODUCTION

The present high level *ab initio* study of iron oxide, FeO, and its ions FeO^+ and FeO^-, is a continuation of our previous works on $VO^{0,\pm}$ (Ref. 1) and $ScO^{0,\pm}$, $TiO^{0,\pm}$, $CrO^{0,\pm}$, and $MnO^{0,\pm}$ (Ref. 2). The computational difficulties of 3*d*-transition metals (M) containing compounds are well known[3] (see also Ref. 2 and references cited therein), the main reasons being the high density of states and the high orbital and spin angular momenta of the 3*d*-M atoms. For instance in the case of the Fe atom and within a 2.5 eV energy interval there are eight $^{2S+1}$L atomic terms, namely, ^{5}D, ^{5}F, ^{3}F, ^{5}P, ^{3}P, ^{7}D, ^{3}H, and ^{3}F.[4] Considering only the lowest reaction channel Fe(^{5}D) + O(^{3}P) we get 27 $^{2S+1}\Lambda$ low-lying FeO molecular terms, disregarding their Ω components.

It seems that FeO is one of the most abstruse among the 3*d*-metal oxides (MOs) both experimentally and theoretically. Despite the extensive experimental work on FeO,[5–30] definite, non-conflicting experimental results are limited. For instance, the ground state symmetry of FeO was firmly established relatively recently by Merer and co-workers,[16,17] whereas even the ground state vibrational frequency was not known with certainty until 1997.[27] What we do know experimentally with confidence for FeO are the symmetries of the ground ($X\ ^5\Delta$) and first excited ($A\ ^5\Sigma^+$) states, their bond lengths $r_0 = 1.6194$ (Ref. 26) and 1.6258 Å,[14] and the binding energy $D_0^0 = 96.4 \pm 0.23$ kcal/mol,[29] the harmonic frequency $\omega_e = 882$ cm^{-1},[27] the dipole moment $\mu = 4.50 \pm 0.03$ D,[28] and the electron affinity EA $= 1.492 \pm 0.020$ (Ref. 11) (or 1.495 eV (Ref. 27)) of the $X\ ^5\Delta$ state.

Quantum mechanical *ab initio* calculations on FeO are confined to seven publications.[31–37] It is remarkable, however, that as early as 1973 the first singles and doubles configuration interaction (CISD) calculation with Slater orbitals by Bagus and Preston,[31] predicted correctly the ground state of FeO to be $^5\Delta$. Twelve years later Krauss and Stevens[32] studied by multiconfiguration self-consistent field (MCSCF) some 13 states of FeO (and RuO) around equilibrium employing relativistic effective potentials. Dolg *et al.*[33] calculated through CISD with adjusted *ab initio* pseudopotentials the ground states of the entire MO series, M = Sc–to–Zn. In 1990 Bauschlicher and co-workers[34] studied the dipole moment of the $X\ ^5\Delta$ state of FeO (and TiO, NiH), by multireference (MRCI) and averaged coupled-pair functional (ACPF) methods in conjunction with [6*s*5*p*4*d*3*f*/$_{\rm Fe}$5*s*5*p*2*d*1*f*/$_{\rm O}$] Gaussian basis sets. Perhaps the most thorough calculations up to 1995 are those of Bauschlicher and Maitre,[35] who studied the ground states of the 3*d*-metal oxides and sulfides by multireference ACPF and coupled-cluster, CCSD(T)/[7*s*6*p*4*d*3*f*2*g*/$_{\rm M}$ aug-cc-pVQZ/$_{\rm O,S}$], methods. Their results r_e, ω_e, D_0^0, and μ can be considered, in general, in good agreement with experiment. For the $X\ ^5\Delta$ state of FeO they report (experimental results in parenthesis): $r_e = 1.609$ ($r_0 = 1.6194$ (Ref. 26)) Å, $\omega_e = 885$ (882) cm^{-1},[27] $D_0^0 = 84.2$ (96.4) kcal/mol,[29] and $\mu = 4.17$ (4.5 ± 0.03) D (Ref. 28). However, our results indicate clearly (*vide infra*) that this good agreement of r_e, ω_e, and μ is rather due to error cancellations. Cardoen and Gdanitz[36] investigated the dipole moment of the $X\ ^5\Delta$ state of FeO through ACPF-like multireference and CISD/[6*s*5*p*4*d*3*f*/$_{\rm Fe}$5*s*5*p*2*d*1*f*/$_{\rm O}$] methods at fixed geometry ($r = 1.6404$ Å). Their results for all methods employed deviate from experiment by +0.6 to +0.7 D. The calculation of dipole moments has been proved one of the most difficult and method-sensitive properties; obtaining accurate results and for the right reasons is an arduous task (see also Ref. 38). The case of FeO in particular seems to be by now notorious, while even our present extensive calculations on FeO do not converge to the experimental μ value[28] (*vide infra*).

The most recent *ab initio* work on FeO (and FeO^-) is that of Hendrickx and Anam.[37] These workers examined around equilibrium 12 and 5 states of FeO and FeO^-, respectively, at the multireference perturbation approach, CASPT2/[8*s*7*p*5*d*4*f*2*g*/$_{\rm Fe}$6*s*5*p*4*d*2*f*/$_{\rm O}$], including scalar relativity through the Douglas–Kroll–Hess approximation. For the first three states of FeO, i.e., $X\ ^5\Delta$, $A\ ^5\Sigma^+$, and $a\ ^7\Sigma^+$ (and two for FeO^-), a larger [8*s*7*p*6*d*4*f*2*g*1*h*/$_{\rm Fe}$7*s*6*p*4*d*3*f*1*g*/$_{\rm O}$] basis was also used.[37] For all states they report r_e, ω_e, and T_e; in addition electron affinities (EAs) and dipole moments

a)Electronic mail: mavridis@chem.uoa.gr.

are reported for the $X\ ^5\Delta$, $A\ ^5\Sigma^+$, and $a\ ^7\Sigma^+$ states using the larger basis set. Their results, at least for the first three states, are in acceptable agreement with the present work (see below). Finally, we have traced five density functional theory (DFT) publications on FeO using a variety of functionals.[39–43]

There are nine experimental publications on FeO^+,[10,30,44–50] concerning the ground ($X^6\Sigma^+$) and two excited states, $^6\Pi_{7/2}$ and $^6\Sigma^+$. With confidence we do know the symmetry of the ground state,[48] its binding energy $D_0^0 = 81.2 \pm 0.5$ kcal/mol (Ref. 30) at $r_0 = 1.643 \pm 0.001$ (Ref. 49) (or 1.641 ± 0.001) Å,[50] and its harmonic frequency $\omega_e = 844 \pm 1\ cm^{-1}$.[50] For the $^6\Pi_{7/2}$ and $^6\Sigma^+$ states located 14 351.05 (Ref. 49) and 28 648.7 ± 0.1 cm^{-1} (Ref. 48) higher, $r_0 = 1.900 \pm 0.001$ (Ref. 49) and 1.674 ± 0.005 Å,[48] respectively, and $\omega_e(^6\Sigma^+) = 662 \pm 2\ cm^{-1}$.[48]

We are aware of three *ab initio*[32,51,52] and three DFT (Refs. 53, 52, and 49) publications on FeO^+. Krauss and Stevens[32] reported the first *ab initio* (MCSCF + relativistic effective potentials) calculations, predicting correctly the ground state of FeO^+; they also examined the first three low-lying quartets. In 1993 Fiedler *et al.*[51] studied around equilibrium the $X\ ^6\Sigma^+$ and $^4\Phi$ states of FeO^+ by a variety of methods [QCISD(T), CCSD(T), MRCI, CASPT2] and two basis sets, the larger being $[8s7p4d1f/_{Fe}4s3p2d/_O]$. At the highest level and given the complexity of the FeO^+ system, their results can be considered as fair. Finally Nakao *et al.*[52] studied the entire series of the 3*d*-MO^+s (M = Sc–to–Zn) by MRCI, multireference second-order Møller Plesset (MRMP),[54] and DFT/(B3LYP, BLYP, BOP) methods, using the Stuttgart relativistic small core effective potentials for the metal(s) and the cc-pVTZ basis set for the oxygen atom. For the FeO^+, in addition to the ground state, they also examined around equilibrium five sextets and five quartets of $\Sigma^{\pm}$, Π, Δ, and Φ spatial symmetries at the MRCI level reporting r_e, D_0, and ω_e.[52]

On the FeO^- anion there exist four experimental photoelectron spectrometry publications[11,25,27,55] for two $^4\Delta$ states. According to the experimentalists the ground state of FeO^- is of $^4\Delta$ symmetry[27,55] (but see below), with a second $^4\Delta$ state located ~12 000 cm^{-1} higher.[55] All the experimental results on FeO^- are summarized later on in Sec. III C.

Theoretical *ab initio* work on FeO^- is limited to three publications dealing with the $^4\Delta$, $^6\Sigma^-$, $^6\Delta$, $^6\Pi$, and $^4\Pi$ states studied around equilibrium.[33,37,43] The most recent calculations are those of Hendrickx and Anam[37] at the CASPT2 level (*vide supra*). Surprisingly, these workers concluded that the ground state of FeO^- is of $^6\Sigma^+$ symmetry with a $^4\Delta$ state located 1049 cm^{-1} higher, disputing the experimental results of Andersen *et al.*;[55] see also the commentary by Neumark and Lineberger[56] strongly doubting the conclusions of Hendrickx and Anam.[37] It should be added at this point, however, that our very large calculations support, at least formally, that the FeO^- ground state is $^6\Sigma^+$ (*vide infra*).

The above summary, on the experimental and theoretical work on FeO and $FeO^{\pm}$, shows the need for a systematic and extensive theoretical work on these species. Employing variational multireference and single reference coupled-cluster calculations combined with large correlation consistent basis sets, we have examined 48 (FeO), 24 (FeO^+), and 4 (FeO^-) bound states, reporting full potential curves (PECs), spectroscopic parameters (r_e, ω_e, $\omega_e x_e$, α_e) dissociation energies (D_e), dipole moments (μ), separation energies (T_e), and spin orbit (SO) coupling constants. The paper is organized as follows: in Sec. II we outline the methods and basis sets, results and discussion on FeO, FeO^+, and FeO^- are presented in Secs. III A–III C, whereas in Sec. IV we give the SO coupling constants; final conclusions and remarks are epitomized in Sec. V.

II. BASIS SETS AND METHODS

Correlation consistent (cc) basis sets were used throughout the whole study.[57] For the Fe atom the cc-basis set of quintuple cardinality by Balabanov and Peterson was employed,[58] combined with the quintuple augmented basis set aug-cc-pV5Z for the O atom.[57,59] Both sets were generally contracted to $[9s8p6d4f3g2h1i/_{Fe}7s6p5d4f3g2h/_O] = A5\zeta$. The A5$\zeta$ basis was used for the construction of all PECs of the present study. When the Fe core (subvalence) $3s^23p^6$ electrons were included in the CI calculations the A5ζ basis was extended by a set of weighted core functions $(2s2p2d1f1g1h1i)$,[58] resulting to a contracted basis set $[11s10p8d5f4g3h2i/_{Fe}7s6p5d4f3g2h/_O] = CA5\zeta$ of order 338.

All molecular states have been calculated by the complete active space self-consistent field (CASSCF) + single + double replacements (CASSCF + 1 + 2 = MRCI) method under C_{2v} restrictions. Certain low lying states, whenever possible, were also studied through the restricted coupled-cluster + singles + doubles + quasi-perturbative connected triples approach, RCCSD(T).[60] Because of convergence problems at the Hartree–Fock level natural CASSCF orbitals were used in all RCCSD(T) calculations. The CASSCF reference functions are defined by allotting 12 (FeO), 11 (FeO^+), and 13 (FeO^-) electrons to nine "valence" orbitals ($4s + 3d/_{Fe} + 2p/_O$), respectively. Corresponding (valence) internally contracted (ic) (Ref. 61) wave functions were calculated through single and double excitations out of the reference spaces including the complete valence space of the O atom ($2s2p$). For a few low-lying states core correlation effects were taken into account by including the $3s^23p^6$ electrons of the Fe atom in the MRCI and RCCSD(T) calculations, named C − MRCI and C − RCCSD(T), respectively. In addition, larger valence MRCI calculations (MRCI − L) have been performed for a few low lying states, by including the three 4*p* (Fe) and the one 2*s* (O) orbitals in the reference space. To make these MRCI − L calculations feasible we were forced to restrict the CASSCF excitations to no more than singles and doubles to the 4*p* space. The icC − MRCI (C − MRCI) expansions, for the $X\ ^5\Delta$ state of FeO for instance, contain 11.6×10^6 (1.7×10^9) configuration functions (CF) as contrasted to 1.5×10^6 (234×10^6) CFs of the icMRCI (MRCI) expansions. On the other hand the icMRCI − L (MRCI − L) expansions range from 20×10^6 (2.6×10^9) CFs for the $^7\Sigma^+$ of FeO to 78×10^6 (11×10^9) CFs for the $^4\Delta$ state of FeO^-.

Scalar relativistic effects for the first few states were taken into account through the second-order Douglas–Krol–Hess (DKH2) (Refs. 62 and 63) Hamiltonian using the A5ζ and CA5ζ basis sets recontracted accordingly.[58] Spin–orbit

couplings were estimated by diagonalizing the $\hat{H}_e + \hat{H}_{SO}$ Hamiltonian within the $\hat{H}_e$ icMRCI/A5ζ eigenvectors, where the $\hat{H}_{SO}$ is the full Breit–Pauli operator. Basis set superposition errors (BSSEs) obtained by the counterpoise method[64] are less than 0.4 kcal/mol at the MRCI or RCCSD(T) methods for the $X\,^5\Delta$ state of FeO. The BSSE is considered to be constant (= 0.4 kcal/mol) for all states studied. Spectroscopic parameters were obtained by solving numerically the one-dimensional ro-vibrational Schrödinger equation.

Non-extensivity errors (NEs) are estimated by subtracting the sum of the energies of the individual atoms from the total energies of the corresponding supermolecule at r_{Fe-O} = 30 bohr. For the $X\,^5\Delta$ state of FeO NE = 18(7) and 31(11) mE_h at the icMRCI(+Q)/A5ζ and icC − MRCI(+Q)/CA5ζ levels, respectively, where +Q is the Davidson correction.[65] Corresponding NEs at the (multireference) averaged coupled-pair functional (ACPF) (Ref. 66) level are 0.5 (ACPF/A5ζ) and 0.6 (C− ACPF/CA5ζ) mE_h. All calculations were performed by the MOLPRO suite of codes.[67]

III. RESULTS AND DISCUSSION

A. FeO

The ground state of Fe is ^{5}D ($4s^13d^6$) with the first two excited states ^{5}F ($4s^13d^7$) and ^{3}F ($4s^13d^7$), 0.875 and 1.488 eV (M_J averaged) higher.[4] The interaction of Fe (^{5}D, ^{5}F, ^{3}F) + O(^{3}P) gives rise to 27, 36, and 36 $^{2S+1}\Lambda$ molecular terms, namely,[7,5,3](Φ, Δ[2], Π[3], Σ^+, Σ^-[2]), [7,5,3](Γ, Φ[2], Δ[3], Π[3], Σ^+[2], Σ^-), and [5,3,1](Γ, Φ[2], Δ[3], Π[3], Σ^+[2], Σ^-), respectively. We have studied all 27 states which correlate adiabatically to the first channel (^{5}D + ^{3}P), 14 to the second (^{5}F + ^{3}P), and 8 singlets correlating to the third channel (^{3}F + ^{3}P), a total of 49 states within an energy range of ~3 eV. Full MRCI/A5ζ PECs have been constructed for the 49 states considered, all of which but one ($2\,^7\Sigma^-$) are bound with respect to their adiabatic fragments (from now on by MRCI it is meant icMRCI). The interaction, however, of Fe(^{5}D; $4s^23d^6$) + O(^{3}P) is of repulsive nature due primarily to the much larger radius of the Fe 4s electron distribution (r_{4s}) as compared to its 3d (r_{3d}), the Hartree–Fock $\langle r_{4s}\rangle/\langle r_{3d}\rangle$ ratio being close to 3.[68] Therefore, it is more convenient to consider the FeO molecule as ionic, considering that according to our results 0.6–0.7 e$^-$ are transferred from Fe to the O atom (*vide infra*). The $^{2S+1}\Lambda$ molecular states of FeO obtained from the first two ionic channels Fe^+ [^{6}D ($4s^13d^6$), ^{4}F ($3d^7$)] + O^- (^{2}P)] are [7,5](Φ, Δ[2], Π[3], Σ^+, Σ^-[2]) and [5,3](Γ, Φ[2], Δ[3], Π[3], Σ^+, Σ^-[2]), respectively, a total of 42 states triplets, quintets, and septets; experimentally $\Delta E(^4\text{F} - {}^6\text{D})$ = 0.248 eV.[4]

Tables I and II list numerical results (E, r_e, D_e, ω_e, $\omega_e x_e$, α_e, μ, T_e) for 48 bound states of FeO along with experimental findings for easy comparison, while Fig. 1 displays the corresponding MRCI + Q/A5ζ PECs and their energy level diagram (inset).

1. $X\,^5\Delta$

As was mentioned in the introduction the experimental ground state of FeO is $X\,^5\Delta$[16,17] with a $A\,^5\Sigma^+$ state

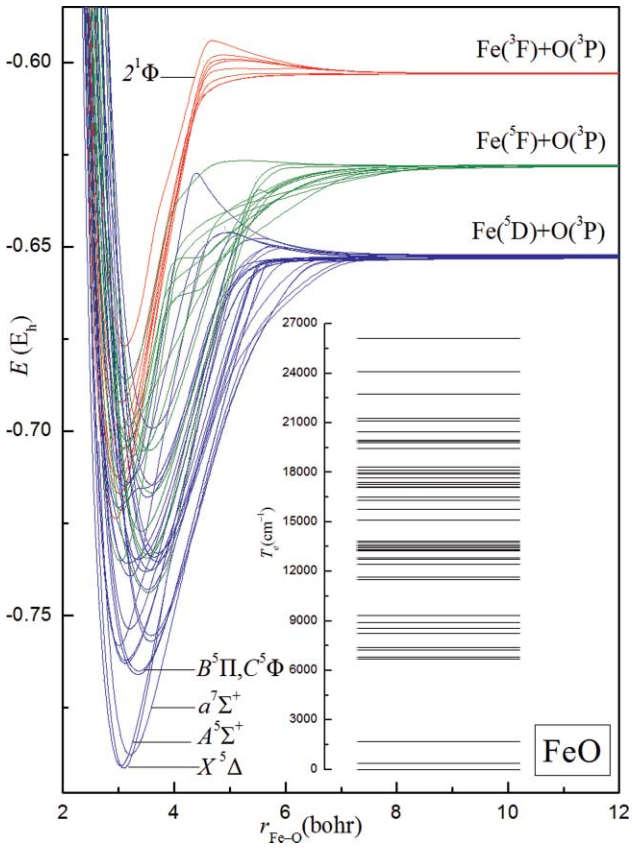

FIG. 1. MRCI + Q/A5ζ adiabatic PECs and energy level diagram (inset) of 48 bound states of FeO. The ordering follows that of Tables I–II. All energies are shifted by +1337 E_h.

~4000 cm^{-1} higher.[23,25,27] Although our results indicate that, formally, $a\,^5\Delta$ state can be adopted as the lowest state of FeO, it is practically degenerate with the $A\,^5\Sigma^+$ state. As a matter of fact, the C − ACPF + DKH2 approach predicts an inverse order than the experimental one by 1350 cm^{-1}; see Table I. At all levels of theory the subvalence ($3s^23p^6$) core effects of Fe seem to increase the $^5\Sigma^+ - X\,^5\Delta$ separation by ~500 cm^{-1}. Therefore, assuming similar core effect at the MRCI − L level the sequence of calculations C − MRCI + DKH2 + Q, C − ACPF + DKH2, C − RCCSD(T) + DKH2 and C − MRCI − L + DKH2 + Q predicts $\Delta E(^5\Sigma^+ - X\,^5\Delta)$ = 38, −1350, 1102, −352 + 500 ≈ 150 cm^{-1}, respectively. Similar results, ΔE = 323 cm^{-1}, have been obtained recently by Hendrickx and Anam by the CASPT2 method.[37] This stark disagreement in the $^5\Sigma^+ - X\,^5\Delta$ energy separation between experiment and theory, ~4000 cm^{-1} versus ~300 cm^{-1} or even less, is surprising and indeed interesting deserving further investigation. Nevertheless, independently of the symmetry of the ground state, it is certain that the $X\,^5\Delta$ and $A\,^5\Sigma^+$ states are energetically very close.

At the highest level of the MRCI, ACPF, and RCCSD(T) methods, the bond distance is calculated to be r_e = 1.595 Å, some 0.024 Å shorter than the experimental one. The combined core ($3s^23p^6$) + relativistic effects amount to a bond shortening of ~0.005 + 0.005 = 0.01 Å. Correcting for core effects the MRCI − L + DKH2 + Q results we obtain r_e = 1.611 − 0.005 = 1.606 Å, in relatively good agreement

TABLE I. Total energies E (E_h), bond distances r_e (Å), dissociation energies D_e (kcal mol^{-1}), harmonic frequencies and anharmonicity corrections ω_e, $\omega_e x_e$ (cm^{-1}), rotational–vibrational coupling constants $\alpha_e \times 10^3$ (cm^{-1}), dipole moments μ (D), Mulliken charges on Fe q_{Fe}, and energy separations T_e (cm^{-1}) of the first five states of $^{56}Fe^{16}O$.

Method[a]	$-E$	r_e	D_e[b]	ω_e	$\omega_e x_e$	α_e	$\langle\mu\rangle/\mu_{\mathrm{FF}}$[c]	q_{Fe}	T_e
				$X\,^5\Delta$ (^{5}D)					
MRCI	1337.75477	1.612	81.9	864	7.2	5.1	3.42/4.38	0.60	0.0
MRCI + Q	1337.79630	1.602	86.6	900	7.3	4.9	/4.65		0.0
MRCI + DKH2	1346.69018	1.608	80.3	870	7.4	5.1	3.52/4.36		0.0
MRCI + DKH2 + Q	1346.73225	1.598	85.2	906	7.4	4.9	/4.58		0.0
C − MRCI	1338.15370	1.609	80.3	871	7.9	5.1	3.37/4.24		0.0
C − MRCI + Q	1338.23964	1.597	87.5	916	7.8	4.7	/4.55		0.0
C − MRCI + DKH2	1347.08596	1.606	78.6	874	7.8	5.3	3.49/4.24		0.0
C − MRCI + DKH2 + Q	1347.17215	1.594	85.7	920	7.8	5.0	/4.51		0.0
ACPF	1337.79664	1.605	85.1	893	7.4	4.9	2.93/4.57		0.0
ACPF + DKH2	1346.73270	1.600	83.7	900	7.4	5.0	2.98/4.54		0.0
C − ACPF	1338.24933	1.597	85.4	920	8.0	4.9	2.67/4.52		0.0
C − ACPF + DKH2	1347.18220	1.593	83.9	925	7.9	5.0	2.73/4.48		0.0
RCCSD(T)	1337.81667	1.607	92.2	905	5.9	4.2	/5.41		0.0
RCCSD(T) + DKH2	1346.75192	1.601	90.2	914	6.1	4.4	/5.24		0.0
C − RCCSD(T)	1338.28267	1.601	93.0	919	6.0	4.3	/5.39		0.0
C − RCCSD(T) + DKH2	1347.21437	1.595	90.7	929	6.2	4.5	/5.23		0.0
MRCI − L	1337.77965	1.621	88.3	880	6.3	4.2	4.10/5.58		0.0
MRCI − L + Q	1337.80694	1.616	89.5	902	6.1	3.9	/5.73		0.0
MRCI − L + DKH2	1346.71489	1.615	86.6	884	6.4	4.3	4.12/5.35		0.0
MRCI − L + DKH2 + Q	1346.74241	1.611	87.8	905	6.1	4.0	/5.45		0.0
CASPT2[d]		1.612		887			/4.69		
Expt.		1.6194[e]	96.4[f]	882[g]			4.50 ± 0.03($^5\Delta_4$)[h]		
							4.29 ± 0.05($^5\Delta_3$)[h]		
				$A\,^5\Sigma^+$ (^{5}D)					
MRCI	1337.74979	1.643	78.8	872	4.2	3.6	3.36/4.27	0.55	1093
MRCI + Q	1337.79452	1.635	85.5	899	4.8	3.7	/4.17		391
MRCI + DKH2	1346.68874	1.632	79.4	894	4.8	3.8	3.36/4.21		316
MRCI + DKH2 + Q	1346.73420	1.624	86.4	920	4.9	3.7	/4.07		−427
C − MRCI	1338.14580	1.643	75.3	874	5.2	3.9	3.26/4.33		1733
C − MRCI + Q	1338.23544	1.631	84.8	906	5.4	3.8	/4.30		923
C − MRCI + DKH2	1347.08173	1.632	75.9	891	4.9	3.8	3.26/4.28		928
C − MRCI + DKH2 + Q	1347.17198	1.620	85.6	925	5.1	3.8	/4.20		38
ACPF	1337.80031	1.632	87.4	930	6.3	4.0	3.47/4.13		−806
ACPF + DKH2	1346.74033	1.626	88.5	953	6.9	3.6	3.43/3.97		−1676
C − ACPF	1338.25132	1.628	86.6	942	5.5	4.4	3.32/4.04		−436
C − ACPF + DKH2	1347.18835	1.623	87.7	966	7.3	3.6	3.28/3.90		−1350
RCCSD(T)	1337.80960	1.630	87.7	919	4.4	3.5	/4.40		1551
RCCSD(T) + DKH2	1346.74935	1.619	88.6	938	4.7	3.6	/4.38		562
C − RCCSD(T)	1338.27315	1.631	87.0	916	4.1	3.3	/4.49		2090
C − RCCSD(T) + DKH2	1347.20935	1.619	87.5	931	4.2	3.4	/4.35		1102
MRCI − L	1337.77557	1.640	85.7	900	4.6	3.5	4.45/4.56		897
MRCI − L + Q	1337.80454	1.637	88.0	919	4.4	3.2	/4.31		528
MRCI − L + DKH2	1346.71472	1.630	86.5	912	4.6	3.5	4.29/4.47		37
MRCI − L + DKH2 + Q	1346.74402	1.628	88.8	928	4.2	3.3	/4.23		−352
CASPT2[d]		1.626		868			/3.61		323
Expt.		1.6258[i]		881[i]					3780 ± 120[j]
				800[g]					3871 ± 161[k]
									4050[g]
				$a\,^7\Sigma^+$ (^{5}D)					
MRCI	1337.74997	1.696	78.9	752	5.2	4.6	2.22/2.41	0.62	1053
MRCI + Q	1337.78855	1.685	81.8	779	5.9	4.9	/2.38		1701
MRCI + DKH2	1346.68672	1.685	78.2	766	5.4	4.8	2.28/2.49		759
MRCI + DKH2 + Q	1346.72604	1.674	81.3	797	6.3	5.0	/2.48		1362
C − MRCI	1338.14709	1.702	76.2	740	4.7	4.5	2.26/2.41		1451
C − MRCI + Q	1338.22922	1.688	81.0	768	5.4	4.7	/2.39		2288
C − MRCI + DKH2	1347.08064	1.692	75.3	751	4.9	4.7	2.31/2.48		1168
C − MRCI + DKH2 + Q	1347.16324	1.678	80.2	783	5.7	4.9	/2.48		1954

TABLE I. (*Continued.*)

Method[a]	$-E$	r_e	D_e[b]	ω_e	$\omega_e x_e$	α_e	$\langle\mu\rangle/\mu_{FF}$[c]	q_{Fe}	T_e
ACPF	1337.78981	1.683	80.8	786	6.2	5.0	1.98/2.32		1497
ACPF + DKH2	1346.72756	1.671	80.5	807	6.7	5.1	2.00/2.42		1127
C − ACPF	1338.23912	1.683	79.1	781	6.0	5.0	1.94/2.27		2241
C − ACPF + DKH2	1347.17367	1.671	78.6	800	6.4	5.1	1.94/2.37		1873
RCCSD(T)	1337.80095	1.666	82.3	865	8.7	4.9	/2.44		3451
RCCSD(T) + DKH2	1346.73957	1.660	82.5	884	8.6	4.8	/2.55		2710
C − RCCSD(T)	1338.26293	1.666	80.6	870	7.9	4.6	/2.37		4334
C − RCCSD(T) + DKH2	1347.19829	1.659	80.6	886	7.8	4.6	/2.48		3531
MRCI − L	1337.77294	1.689	84.2	801	7.2	4.7	2.41/2.47		1475
MRCI − L + Q	1337.79901	1.685	84.8	824	7.5	4.5	/2.46		1742
MRCI − L + DKH2	1346.71073	1.681	84.0	825	7.5	4.5	2.55/2.57		913
MRCI − L + DKH2 + Q	1346.73720	1.678	84.5	847	7.6	4.3	/2.55		1144
CASPT2[d]		1.677		756			/2.78		1936
Expt.				877[g]					∼2100[l]
									1144[g]
				B $^5\Pi$ (^{5}**D**)					
MRCI	1337.73099	1.791	66.9	577	1.2	2.3	1.96/2.04	0.61	5219
MRCI + Q	1337.76573	1.778	67.4	565	0.6	2.6	/1.88		6710
MRCI + DKH2	1346.66619	1.782	65.2	576	1.0	2.5	1.96/2.05		5264
MRCI + DKH2 + Q	1346.70143	1.767	65.8	563	0.2	2.8	/1.88		6765
C − MRCI	1338.13138	1.787	66.1	584	1.3	2.3	2.03/2.09		4897
C − MRCI + Q	1338.20987	1.768	68.7	573	0.6	2.7	/1.91		6534
C − MRCI + DKH2	1347.06360	1.778	64.3	583	1.0	2.5	2.03/2.09		4909
C − MRCI + DKH2 + Q	1347.14235	1.759	66.9	571	0.1	3.0	/1.92		6541
MRCI − L	1337.74691	1.778	67.7	570	1.5	2.7	1.72/1.83		7187
MRCI − L + Q	1337.77142	1.757	67.3	575	1.2	3.1	/1.69		7795
MRCI − L + DKH2	1346.68240	1.767	66.2	569	1.2	2.9	1.72/1.86		7130
MRCI − L + DKH2 + Q	1346.70736	1.745	65.8	575	0.9	3.4	/1.70		7693
Expt.		1.735[m]		∼610[m]					∼8500[l]
				630[n]					10 200[n]
				C $^5\Phi$ (^{5}**D**)					
MRCI	1337.73062	1.793	66.6	577	1.2	2.3	1.96/2.04	0.61	5299
MRCI + Q	1337.76526	1.780	67.1	566	0.6	2.6	/1.88		6811
MRCI + DKH2	1346.66579	1.784	64.9	576	1.0	2.5	1.96/2.04		5352
MRCI + DKH2 + Q	1346.70091	1.769	65.5	564	0.3	2.8	/1.87		6879
C − MRCI	1338.13102	1.788	65.9	584	1.2	2.3	2.03/2.08		4977
C − MRCI + Q	1338.20937	1.771	68.4	574	0.7	2.7	/1.91		6643
C − MRCI + DKH2	1347.06321	1.780	64.1	582	1.0	2.4	2.04/2.09		4994
C − MRCI + DKH2 + Q	1347.14180	1.762	66.6	572	0.2	3.0	/1.92		6661
MRCI − L	1337.74639	1.782	67.4	575	1.6	2.8	1.72/1.80		7301
MRCI − L + Q	1337.77071	1.764	66.9	582	1.4	3.2	/1.66		7952
MRCI − L + DKH2	1346.68180	1.772	65.7	573	1.4	3.0	1.73/1.80		7261
MRCI − L + DKH2 + Q	1346.70652	1.753	65.2	582	1.3	3.4	/1.62		7878
Expt.		1.735[m]		∼610[m]					∼8500[l]
		1.731[o]							10 185[o]

[a]+Q, DKH2, and C− refer to the Davidson correction for unlinked clusters, Douglas–Kroll–Hess approximation of second order for scalar relativity, and that the sub-valence core electrons of Fe($3s^2 3p^6$) have been included in the CI calculations. Calculations marked by "−L" (MRCI − L, MRCI + Q − L, MRCI + DKH − L, MRCI + DKH + Q − L) have been performed with a much larger reference space; see text.

[b]With respect to adiabatic products; values in parentheses after the molecular term symbol denote the end term symbol of Fe.

[c]Dipole moment calculated as an expectation value $\langle\mu\rangle$, or through the finite-field approach, μ_{FF}; field strength 10^{-5} a.u.

[d]Reference 37.

[e]Reference 26; rotational spectroscopy, r_0 value.

[f]Reference 29; velocity map imaging photodissociaiton, D_0^0 value.

[g]Reference 27; zero kinetic energy photoelectron spectroscopy.

[h]Reference 28; optical Stark spectroscopy.

[i]Reference 14; vibrational spectroscopy; r_0 value. It is assumed that $^5\Sigma^+$ is the ground state.

[j]Reference 23; photoelectron spectroscopy (PES).

[k]Reference 25; PES.

[l]Reference 19; Fourier transform spectroscopy.

[m]Reference 24; laser induced fluorescence spectrometry, r_0 and $\Delta G_{1/2}$ ($= \omega_e - 2\omega_e x_e$) values.

[n]Reference 17; LIFS and discharge emission spectroscopy.

[o]Reference 17; mean values of the $C^5\Phi_\Omega$ components, $\Omega = 1$–5. r_0 values range from 1.712 Å ($^5\Phi_1$) to 1.746 Å ($^5\Phi_5$) while T_0 values range from 10 446 cm^{-1} ($^5\Phi_1$) and 9904 cm^{-1} ($^5\Phi_5$).

TABLE II. MRCI + Q total energies E (E_h), bond distances r_e (Å), dissociation energies D_e (kcal mol^{-1}), harmonic frequencies and anharmonicity corrections ω_e, $\omega_e x_e$ (cm^{-1}), rotational–vibrational coupling constants $\alpha_e \times 10^3$ (cm^{-1}), dipole moments μ (D), Mulliken charges on Fe q_{Fe}, and energy separations T_e (cm^{-1}) of higher states of ^{56}Fe^{16}O.

State[a]	$-E$	r_e	D_e[b]	ω_e	$\omega_e x_e$	α_e	μ_{FF}	q_{Fe}	T_e
$1\,^3\Phi\,(^5\mathrm{D})$	1337.76326	1.648	69.1	678	3.7	5.9	3.33	0.47	7252
$1\,^3\Pi\,(^5\mathrm{D})$	1337.76251	1.647	68.7	675	4.2	6.1	3.29	0.48	7416
$1\,^3\Delta\,(^5\mathrm{D})$	1337.75876	1.590	66.7	964	19.9	7.8	3.38	0.55	8238
Expt.				800 ± 60[c,d]					8549 ± 161[c]
									8310 ± 120[d]
$1\,^7\Phi(^5\mathrm{D})$	1337.75725	1.891	65.4	622	3.3	2.9	2.18	0.64	8571
$1\,^7\Pi\,(^5\mathrm{D})$	1337.75570	1.894	64.5	618	3.2	2.9	2.26	0.65	8910
$2\,^5\Pi\,(^5\mathrm{D})$	1337.75376	1.695	63.3	724 ($= \Delta G_{1/2}$)			4.14	0.68	9336
$2\,^5\Sigma^+\,(^5\mathrm{F})$	1337.74394	1.869	72.8	550 ($= \Delta G_{1/2}$)			2.53	0.67	11 492
$2\,^5\Delta\,(^5\mathrm{D})$	1337.74314	1.859	57.2	583 ($= \Delta G_{1/2}$)			2.60	0.67	11 667
$2\,^3\Delta\,(^5\mathrm{D})$	1337.73964	1.704	54.9	747 ($= \Delta G_{1/2}$)			3.62	0.55	12 436
$3\,^5\Pi\,(^5\mathrm{D})$	1337.73817	1.832	53.7	576 ($= \Delta G_{1/2}$)			2.28	0.74	12 757
$1\,^5\Sigma^-\,(^5\mathrm{D})$	1337.73786	1.888	53.7	575	3.5	2.6	2.73	0.68	12 827
$1\,^3\Sigma^-\,(^5\mathrm{D})$	1337.73604	1.671	52.5	509 ($= \Delta G_{1/2}$)			4.31	0.56	13 227
$1\,^3\Gamma\,(^5\mathrm{F})$	1337.73579	1.598	67.7	907	4.6	4.1	4.08	0.49	13 280
$1\,^7\Delta\,(^5\mathrm{D})$	1337.73559	1.947	52.2	575	3.6	2.6	3.01	0.70	13 325
$1\,^3\Sigma^+\,(^5\mathrm{D})$	1337.73505	1.776	51.8	557	6.1	0.4	3.31	0.58	13 443
$2\,^5\Phi\,(^5\mathrm{F})$	1337.73470	1.853	66.9	641	3.2	2.9	3.13	0.62	13 519
$2\,^7\Pi\,(^5\mathrm{D})$	1337.73435	1.924	51.0	565	3.1	3.2	2.47	0.62	13 597
$4\,^5\Pi\,(^5\mathrm{F})$	1337.73366	1.858	66.2	632 ($= \Delta G_{1/2}$)			3.18	0.63	13 748
$1\,^7\Sigma^-\,(^5\mathrm{D})$	1337.73328	1.956	50.8	575	3.2	2.8	3.09	0.71	13 831
$3\,^5\Sigma^+\,(^5\mathrm{F})$	1337.72743	1.796	62.6	649	4.2	4.5	2.76	0.73	15 115
$1\,^1\Sigma^+\,(^3\mathrm{F})$	1337.72448	1.556	76.3	1035	3.8	2.9	3.47	0.34	15 763
$3\,^3\Delta\,(^5\mathrm{F})$	1337.72207	1.611	59.1	904	3.6	4.9	3.59	0.49	16 291
$2\,^3\Pi\,(^5\mathrm{D})$	1337.72117	1.589	42.7						16 488
Expt.[c]									$15\,244 \pm 242$
$2\,^3\Sigma^+\,(^5\mathrm{F})$	1337.71850	1.625	56.8	1003	12.3	5.1	3.42	0.50	17 074
$2\,^7\Delta\,(^5\mathrm{D})$	1337.71820	1.859	41.5	639	2.0	4.3	2.18	0.73	17 140
$1\,^1\Phi\,(^3\mathrm{F})$	1337.71754	1.591	71.9	935	4.5	3.8	3.31	0.36	17 285
$3\,^5\Delta\,(^5\mathrm{F})$	1337.71697	1.895	56.0	599	7.4	0.7	3.33	0.66	17 410
Expt.[e]							$2.53 \pm 0.04(^5\Delta_4)$		16 886
							$2.58 \pm 0.06(^5\Delta_3)$		
$3\,^3\Pi\,(^5\mathrm{D})$	1337.71574	1.648	39.5						17 681
$2\,^5\Sigma^-\,(^5\mathrm{D})$	1337.71482	1.905	39.4	601	3.0	2.8	3.40	0.67	17 884
$2\,^3\Sigma^-\,(^5\mathrm{D})$	1337.71446	1.682	39.1	846	0.1	0.9	2.99	0.54	17 962
$1\,^1\Gamma\,(^3\mathrm{F})$	1337.71370	1.596	69.5	923	5.5	4.0	2.71	0.47	18 129
$1\,^1\Pi\,(^3\mathrm{F})$	1337.71287	1.568	69.0	950	5.2	4.2	3.28	0.40	18 311
$4\,^3\Pi\,(^5\mathrm{F})$	1337.70765	1.728	49.8						19 456
$1\,^1\Delta\,(^3\mathrm{F})$	1337.70612	1.597	64.8	937	7.6	4.3	3.23	0.47	19 792
$4\,^5\Delta\,(^5\mathrm{F})$	1337.70577	1.807	49.0	757	7.6	5.3	3.07	0.70	19 869
$2\,^7\Sigma^+\,(^5\mathrm{F})$	1337.70541	1.880	48.6	608	3.7	3.3	2.56	0.74	19 949
$2\,^3\Phi\,(^5\mathrm{F})$	1337.70303	1.666	46.9	792	1.9	3.2	1.39	0.49	20 471
$1\,^1\Sigma^-\,(^3\mathrm{F})$	1337.70003	1.602	61.0	895	6.3	4.4	2.11	0.48	21 130
$3\,^7\Pi\,(^5\mathrm{D})$	1337.69947	1.907	29.4	583	4.9	3.4	2.73	0.78	21 253
$5\,^3\Pi\,(^5\mathrm{F})$	1337.69940	1.682	44.8	1014	20.7	6.2	1.54	0.49	21 267
$2\,^1\Pi\,(^3\mathrm{F})$	1337.69273	1.611	56.3	832	4.6	4.6	1.83	0.43	22 730
$3\,^3\Phi\,(^5\mathrm{F})$	1337.68651	1.656	36.8	792	4.0	4.2	0.89	0.48	24 095
$2\,^1\Phi\,(^3\mathrm{F})$	1337.67740	1.644	46.9	836	0.8	3.0	0.60	0.47	26 095

[a]For MRCI results see supplementary Table S1, Ref. 72.
[b]With respect to adiabatic products; values in parentheses after the molecular term symbol denote the end term symbol of Fe.
[c]Reference 25; PES.
[d]Reference 24; laser induced fluorescence spectrometry, $\Delta G_{1/2}$ ($= \omega_e - 2\omega_e x_e$) values.
[e]Reference 28; optical Stark spectroscopy.

with the experimental r_0 value of 1.6194 Å.[26] Our results, however, concerning the dissociation energy are not very satisfactory. Disregarding the BSSE (~0.4 kcal/mol), D_e ($D_0 = D_e - \omega_e/2$) = 85.7 (84.3), 83.9 (82.6), and 90.7 (89.4) kcal/mol at the C − MRCI + DKH2 + Q, C − ACPF + DKH2, and C − RCCSD(T) + DKH2 levels, respectively, as compared to the experimental value $D_0 = 96.4$ kcal/mol.[29] At the MRCI − L + DKH2 + Q (and correcting by ~+1 kcal/mol due to core effects), $D_e(D_0) = 88.8(87.5)$ kcal/mol, about 9 kcal/mol (~10%) less than the experimental number.

In an effort to improve our D_e (D_0) results we repeated the above calculations using the analogous quadruple basis sets (AQζ), and then we extrapolated to the complete basis set limit through the formula $P = P_{CBS} - A/l^3$, where P is a property, A is a fitting parameter, and l is the cardinality of the basis set;[69] see also Ref. 70 and references therein. At all methods the dissociation energy increases by ~0.3 kcal/mol, a marginal improvement just cancelling the BSSE effect.

We would like to discuss now our findings on the dipole moment of the $X\ ^5\Delta$ state of FeO. The experimental value reported for the first time by Steimle *et al.*[21] is $\mu(X\ ^5\Delta_2) = 4.7 \pm 0.2$ D. Fifteen years later Steimle and co-workers[28] measured the dipole moment of the $\Omega = 3$ and 4 components of the $X\ ^5\Delta$ state reporting $\mu = 4.29 \pm 0.05$ and 4.50 ± 0.03 D, respectively. Our results are, at least, worth discussing. Notice first that expectation value ($\langle\mu\rangle$) versus finite field (μ_{FF}) dipole moments differ significantly, the latter being larger by 1.0–1.5 D and certainly more reliable than the former.[38] At the C − MRCI + DKH2 + Q (C − ACPF + DKH2) level, $\mu_{FF} = 4.51$ (4.48) D, in complete agreement with the experimental dipole moment(s) μ_Ω averaged over the Ω values, $\bar{\mu} = 4.50$ D. Similar theoretical results have been obtained at the CASPT2 level of theory;[37] see Table I. Core and scalar relativistic effects combined reduce the dipole moment by ~0.1–0.2 D depending on the method. However, at the C − RCCSD(T) + DKH2 and MRCI − L + DKH2 + Q levels $\mu_{FF} = 5.23$ and 5.45 D, respectively. Reducing the latter by ~0.1 D (core effects at the MRCI level), μ_{FF} (C − MRCI − L + DKH2 + Q) = 5.3 D, ~0.8 D larger than the experimental value of Steimle *et al.*[28]

Considering the large size of the present calculations, our results [$\Delta E(A\ ^5\Sigma^+ - X\ ^5\Delta)$, D_0, μ_{FF}] are not in satisfactory agreement with experiment, indicating clearly the difficulties of obtaining "right values for the right reasons" for certain molecules like FeO, always assuming, of course, the validity of the experimental results. We turn now to the bonding nature of the $X\ ^5\Delta$ state. The leading equilibrium MRCI configuration and the corresponding Mulliken distributions are (the 20 $1s^2 2s^2 2p^6 3s^2 3p^6/_{Fe} 1s^2/_O$ core electrons have been suppressed)

$$|X^5\Delta\rangle_{A_1} \approx 0.85\left|1\sigma^2 2\sigma^2 3\sigma^1 1\pi_x^2 1\pi_y^2 2\pi_x^1 2\pi_y^1 1\delta_+^2 1\delta_-^1\right\rangle$$
$$4s^{0.87} 4p_z^{0.14} 4p_x^{0.05} 4p_y^{0.05} 3d_{z^2}^{0.97} 3d_{xz}^{1.15} 3d_{yz}^{1.15} 3d_{x^2-y^2}^{1.98} 3d_{xy}^{1.00}$$
$$2s^{1.88} 2p_z^{1.11} 2p_x^{1.77} 2p_y^{1.77}.$$

A total of 0.60 e^- are transferred from the metal to the O atom indicating a strong Coulombic interaction close to equilibrium. Adiabatically the $X\ ^5\Delta$ state correlates to the ground state atoms Fe(^{5}D) + O(^{3}P), but diabatically to Fe^+(^{6}D) and O^-(^{2}P), where the prevailing ionic bond character is due to an avoided ionic-covalent crossing around 5 bohr. Before the avoided crossing, Fe(^{5}D) + O(^{3}P), 3 e^- are shared between the $3d_{xz}$ and $3d_{yz}$ atomic orbitals of Fe and another 3 between the $2p_x$ and $2p_y$ of the O atom. After the avoided crossing and close to equilibrium about 0.5 e^- is transferred from Fe to O through the π frame and ~0.1 through the σ frame. The bonding can be captured by a valence-bond-Lewis (vbL) icon in conformity with the leading configuration and the population analysis.

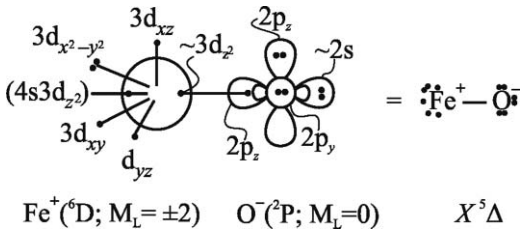

The covalent part of the bond is manifested through the 2σ orbital whose MRCI composition is $2\sigma \approx (0.73)2p_z - (0.55)3d_{z^2} - (0.21)4s$, while the 3σ singly occupied orbital is a hybrid localized on Fe, $3\sigma \approx (0.83)4s - (0.47)3d_{z^2} - (0.35)4p_z$; the 1σ is entirely the $2s$ atomic orbital of the O atom. Assuming that the total Mulliken Fe–to–O charge transfer of 0.60 e^- is close to reality, the bonding in the $X\ ^5\Delta$ state can be thought of as a 80% (~75 kcal/mol = $0.60^2/r_e$) and 20% (~20 kcal/mol) mixture of Coulombic and covalent character, respectively.

2. $A\ ^5\Sigma^+$

As was already discussed the $A\ ^5\Sigma^+$ state is predicted degenerate to the $X\ ^5\Delta$ within the accuracy of our calculations, whereas the experimental T_e is near 0.5 eV; see Table I and Fig. 1. The sequence of higher level calculations C − MRCI + DKH2 + Q (C − ACPF + DKH2) [C − RCCSD(T) + DKH2] gives $r_e = 1.620$ (1.623) [1.619] Å in quite good agreement with the experimental r_0 value of 1.6258 Å.[14] Core effects reduce on the average the bond distance by ~0.003 Å, therefore at the C − MRCI − L + DKH2 + Q level we get $r_e = 1.628 - 0.003 = 1.625$ Å in excellent agreement with experiment. The calculated dipole moment of the $A\ ^5\Sigma^+$ state is practically method invariant converging to $\mu_{FF} = 4.20$ (C − MRCI + DKH2 + Q), 4.35 (C − RCCSD(T) + DKH2), and 4.23 (MRCI − L + DKH2 + Q) D, or correcting the latter value by ~+0.1 D due to the $3s^2 3p^6$ subvalence effects, we suggest a value of 4.3 D, larger by 0.7 D than the CASPT2 value.[37]

The main equilibrium MRCI CF and Mulliken populations are

$$|A^5\Sigma^+\rangle \approx 0.82|1\sigma^2 2\sigma^2 3\sigma^2 1\pi_x^2 1\pi_y^2 2\pi_x^1 2\pi_y^1 1\delta_+^1 1\delta_-^1\rangle$$
$$4s^{1.17} 4p_z^{0.14} 4p_x^{0.04} 4p_y^{0.04} 3d_{z^2}^{1.44} 3d_{xz}^{1.29} 3d_{yz}^{1.29} 3d_{x^2-y^2}^{1.00} 3d_{xy}^{1.00}$$
$$/2s^{1.88} 2p_z^{1.32} 2p_x^{1.64} 2p_y^{1.64}.$$

The $A\ ^5\Sigma^+$ state correlates adiabatically to the ground state atoms, around equilibrium; however, the molecule is fairly ionic with a Mulliken Fe–to–O charge transfer close to 0.6 e^-. The bonding is not very clear; as in the $X\ ^5\Delta$ state after the avoided crossing ~0.3 e^- are transferred from the $3d_\pi$ Fe orbitals to the $2p_\pi$ orbitals of the O atom, and another 0.3 e^- via the σ frame to the singly occupied $2p_z$ orbital. Along the σ frame four electrons are distributed:

$(4s4p_z3d_{z^2})^{1.17+0.14+1.44} + (2p_z)^{1.32}$. The bonding can be described approximately by the diagram below.

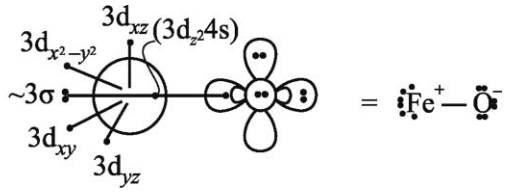

Fe$^+$(^{6}D; M$_L$= 0) O$^-$(^{2}P; M$_L$=0) $A\,^5\Sigma^+$

The MRCI 3σ orbital is to a large extent a $4s3d_{z^2}$ hybrid localized on the metal, $3\sigma \approx (0.71)3d_{z^2} - (0.64)4s + (0.24)4p_z$, whereas the $2\sigma \approx (0.44)3d_{z^2} + (0.28)4s - (0.77)2p_z$, describes a rather weak covalent bond reinforced by a strong Coulombic interaction. One expects a smaller dipole moment of the $A\,^5\Sigma^+$ than the $X\,^5\Delta$ state due to the $3d_{z^2}^{1.5}$ electron distribution on the back of the metal, and indeed this is the case: $\mu_{FF} = 4.3$ versus 5.3 D at the C − MRCI − L + DKH2 + Q level. Unfortunately, the dipole moment of the $A\,^5\Sigma^+$ is experimentally unknown.

3. $\alpha\,^7\Sigma^+$

This is the second excited state of FeO located 1144 cm^{-1} higher according to the most recent experimental findings.[27] With the exception of the coupled-cluster results our highest level calculations are in relative good agreement with the experimental T_e, ranging from 1954 (C − MRCI + DKH2 + Q), to 1873 (C − ACPF + DKH2), to 1144 (MRCI − L + DKH2 + Q) cm^{-1}; see Table I. The complete agreement of the last value with experiment is certainly coincidental because the subvalence $(3s^23p^6)$ correlation effects are missing.

As before we are dealing with an ionic state, the total Mulliken Fe–to–O charge transfer being ~0.6 e$^-$. The $a\,^7\Sigma^+$ is the high spin analogue of $A\,^5\Sigma^+$. Its leading configuration ($c_0 = 0.89$) is obtained from that of $A\,^5\Sigma^+$ by replacing the $3\sigma^2$ of the latter by $3\sigma^14\sigma^1$. The MRCI − L + DKH2 + Q binding energy converges to $D_e = 84$ kcal/mol at $r_e = 1.678$ Å (MRCI − L + DKH2 + Q), or perhaps slightly shorter due to missing core effects; we recommend $r_e = 1.673$ Å.

The equilibrium MRCI populations

$$4s^{0.90}4p_z^{0.34}4p_x^{0.04}4p_y^{0.04}3d_{z^2}^{1.24}3d_{xz}^{1.40}3d_{yz}^{1.40}3d_{x^2-y^2}^{1.00}3d_{xy}^{1.00}$$
$$/2s^{1.94}2p_z^{1.55}2p_x^{1.53}2p_y^{1.53}$$

indicate a transfer of ~0.5 e$^-$ along the σ frame from Fe to the singly occupied $2p_z$ O orbital, and a small Fe–to–O transfer through the $3d_\pi$–$2p_\pi$ route. The 4 e$^-$ of the σ-frame are distributed to the three σ orbitals given below:

$$2\sigma \approx (0.82)2p_z - (0.42)3d_{z^2},$$
$$3\sigma \approx (0.89)3d_{z^2} - (0.42)2p_z,$$
$$4\sigma \approx (0.92)4s - (0.50)4p_z.$$

Observe that the 4σ orbital is a hybrid localized on the metal.

4. $B\,^5\Pi$, $C^5\Phi$.

These two states are experimentally and theoretically degenerate, experimentally located ~8500 cm^{-1} above the $X\,^5\Delta$ state with $r_0 = 1.735$ Å and $\omega_e \sim 610$ cm^{-1}. All experimental results are from Merer's goup;[17,19,24] see Table I. Of course the labeling B and C is only formal. The first four leading equilibrium MRCI configurations of the $B\,^5\Pi$ state with equal weights and corresponding Mulliken populations are.

$$|B^5\Pi\rangle_{B_1} \approx 0.43|1\sigma^22\sigma^23\sigma^14\sigma^11\pi_x^2\overline{1\pi_y^1}2\pi_x^12\pi_y^11\delta_+^11\delta_-^2\rangle$$
$$- 0.43|1\sigma^22\sigma^23\sigma^14\sigma^1\overline{1\pi_x^1}1\pi_y^22\pi_x^12\pi_y^11\delta_+^21\delta_-^1\rangle$$
$$0.42|1\sigma^22\sigma^23\sigma^14\sigma^11\pi_x^21\pi_y^22\pi_x^11\delta_+^11\delta_-^2\rangle$$
$$- 0.42|1\sigma^22\sigma^23\sigma^14\sigma^11\pi_x^21\pi_y^22\pi_y^11\delta_+^21\delta_-^1\rangle$$
$$4s^{0.90}4p_z^{0.32}4p_x^{0.02}4p_y^{0.02}3d_{z^2}^{1.07}3d_{xz}^{1.02}3d_{yz}^{1.02}3d_{x^2-y^2}^{1.49}3d_{xy}^{1.49}$$
$$/2s^{1.96}2p_z^{1.71}2p_x^{1.50}2p_y^{1.50}.$$

The $C\,^5\Phi$ CFs are identical to those of the $B\,^5\Pi$ but with the signs of the second and fourth configurations reversed and with identical populations. For both states we predict a charge transfer from Fe to O of ~0.6 e$^-$, $D_0 = D_e - \omega_e/2 = 64$ kcal/mol, $r_e = 1.745$ ($B\,^5\Pi$) and 1.753 ($C\,^5\Phi$) Å, and $T_e = 7700$–7900 cm^{-1} at the MRCI − L + DKH2 + Q level. Reducing the bond lengths by ~0.01 Å due to the subvalence effects, $r_e = 1.735$ and 1.743 Å, respectively, in good agreement with experiment (Table I). Notice that the combined core + DKH2 effects reduce the r_e, D_e, and T_e (MRCI + Q vs C − MRCI + DKH2 + Q) by 0.02 Å, 1.5 kcal/mol, and 200 cm^{-1}, respectively. The attractive interaction for both $B\,^5\Pi$ and $C\,^5\Phi$ states can be described by the following vbL diagram in conformity with the populations.

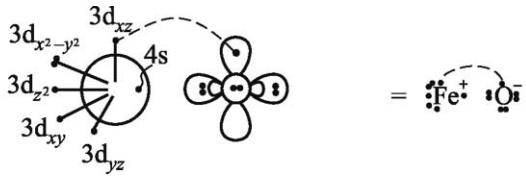

Fe$^+$(^{6}D; M$_L$= ±2) O$^-$(^{2}P; M$_L$= ∓1,±1) $B\,^5\Pi$,$C\,^5\Phi$

The almost pure Coulombic character of the interaction with a Fe–to–O charge transfer of 0.6 e$^-$, predicts a binding energy of ~69 kcal/mol in agreement with the calculated value(s). Finally the recommended dipole moment for both states is $\mu_{FF} = 1.7$ D. Perhaps it is of interest to observe at this point that despite the fact of the same (Mulliken) ionicity of the first five states of FeO, $X\,^5\Delta$, $A\,^5\Sigma^+$, $a\,^7\Sigma^+$, and ($B\,^5\Pi$, $C\,^5\Phi$), their dipole moments decrease monotonically by ~1 D as we move from the X-state to the ($B\,^5\Pi$, $C\,^5\Phi$) pair, 5.3, 4.3, 2.5, and 1.7 D, respectively.

5. Higher states

Table II lists an additional set of 43 states all calculated at the MRCI(+Q)/A5ζ level of theory and lying within an energy range of 19 300 cm^{-1}, or on the average 450 cm^{-1}

per state; see also Fig. 1. Experimental results exist for the $1\ ^3\Delta$,[24,25] $3\ ^5\Delta$,[28] and $2^3\Pi$ (Ref. 25) states calculated to be ~8200, 17 000, and 16 500 cm^{-1} above the $X\ ^5\Delta$ state, in good agreement with experiment; see Table II. However, the calculated dipole moment of the $3\ ^5\Delta$, $\mu_{FF} = 3.3$ D is ~0.7 D larger than the experimental one $\mu = 2.56$ D.[28]

All 43 states, $26 - 5 = 21$ from the first channel ($^5D + {}^3P$), 14 from the second ($^5F + {}^3P$), and 8 from the third ($^3F + {}^3P$), are bound with respect to both adiabatic fragments and to the ground state atoms with MRCI + Q/A5ζ adiabatic binding energies ranging from $D_e = 69$ ($1\ ^3\Phi$) to 47 ($2\ ^1\Phi$) kcal/mol. The 48 states of FeO studied here are quite ionic with increasing ionicity as we move from the singlets (8 states), to the triplets (16 states), to the quintets (15 states), to the septets (9 states), the average positive Mulliken charge on Fe being $\bar{q}_{Fe} = +0.43$, +0.51, +0.65, and +0.69, respectively. Despite the considerable ionic character of all states, $q_{Fe} = 0.55 \pm 0.15$, the variation of the calculated MRCI + Q dipole moments is remarkable, ranging from 4.65 ($X\ ^5\Delta$) to 0.6 ($2\ ^1\Phi$) D.

MRCI results for higher states of FeO are given in supplementary Table S1. The leading MRCI configurations and corresponding atomic populations for 45 states are given in supplementary Tables S2 and S3.[72]

B. FeO^+

The ground state of Fe^+ is $^6D(4s^1 3d^6)$ with the first excited state $^4F(3d^7)$ 0.248 eV higher.[4] The first two channels $Fe^+(^6D, {}^4F) + O(^3P)$ give rise to 27 and 36 $^{2S+1}\Lambda$ states, respectively, namely,[4,6,8](Φ, Δ[2], Π[3], Σ^+, Σ^-[2]) and [2,4,6](Γ, Φ[2], Δ[3], Π[3], Σ^+[2], Σ^-). We have calculated the MRCI+Q/A5ζ PECs for all but one (Σ^-) quartets and 4 sextets [6](Φ, Π[2], Σ^+) correlating adiabatically to the $Fe^+(^6D) + O(^3P)$ channel, and all doublets correlating to the $Fe^+(^4F)$ channel, a total of 24 states. Numerical results for the 24 states are given in Tables III and IV along with existing experimental values and the theoretical MRCI results of Nakao *et al.*[52] for easy comparison; MRCI + Q PECs are displayed in Fig. 2.

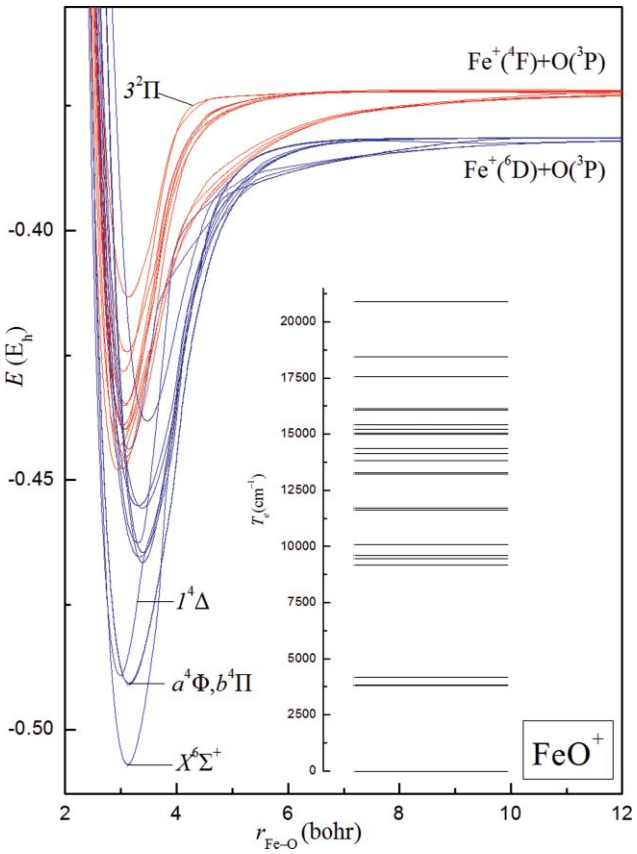

FIG. 2. MRCI + Q/A5ζ adiabatic PECs and level diagram (inset) of 24 states of FeO^+. The ordering follows that of Tables III and IV. All energies are shifted by +1337 E_h.

1. $X\ ^6\Sigma^+$

Some experimental results (r_0, D_0, ω_e) are available for the ground state; however, the entire low-level excited manifold of FeO^+ is in essence uncharted. It is "convenient," and this is quite common, that at the MRCI + Q level our results are practically identical with those at a considerably higher level. As a matter of fact the MRCI + Q r_e and ω_e values are in complete agreement with experiment; see Table III. At the highest level C − MRCI + DKH2 + Q (C − ACPF + DKH2) [C − RCCSD(T) + DKH2], $r_e = 1.629$ (1.630) [1.622] Å, $D_0 (= D_e - \omega_e/2) = 75.6$ (77.4) [76.7] kcal/mol, and $\omega_e = 906$ (905) [884] cm^{-1}, as compared to experimental values $r_0 = 1.643 \pm 0.001$ (Ref. 49) (or 1.641 ± 0.001 Å (Ref. 50)), $D_0 = 81.2 \pm 0.5$ kcal/mol,[30] and $\omega_e = 844\ cm^{-1}$.[50] Core ($3s^2 3p^6$) and scalar relativistic effects reduce the bond distance and dissociation energy by (0.006, 0.01), (0.005, 0.01), (0.004, 0.011) Å, and (2.6, 0.4), (0.9, 0.3), (0.0, 0.3) kcal/mol at the MRCI, ACPF and RCCSD(T) methods, respectively. Notice also that the combined core and relativistic effects are practically additive. Taking into account the core effects at the MRCI − L + DKH2 + Q level we obtain $r_e = 1.628 - 0.006 = 1.622$ Å and $D_0 = 80.0 - 2.6 = 77.4$ kcal/mol, in agreement with our previous results at the highest level of every method, about 0.02 Å shorter and 4 kcal/mol less (~5%) than the experimental values.

The main equilibrium MRCI configuration and corresponding Mulliken distributions are

$$|X^6\Sigma^+\rangle \approx 0.90|1\sigma^2 2\sigma^2 3\sigma^1 1\pi_x^2 1\pi_y^2 2\pi_x^1 2\pi_y^1 1\delta_+^1 1\delta_-^1\rangle$$
$$4s^{0.39} 4p_z^{0.06} 4p_x^{0.03} 4p_y^{0.03} 3d_{z^2}^{1.20} 3d_{xz}^{1.47} 3d_{yz}^{1.47} 3d_{x^2-y^2}^{1.00} 3d_{xy}^{1.00}$$
$$/2s^{1.90} 2p_z^{1.40} 2p_x^{1.47} 2p_y^{1.47}.$$

A total charge of 0.3 e^- is transferred from the $4s3d_{z^2}$ hybrid on Fe^+ to the singly occupied $2p_z$ orbital. By taking also into consideration the composition of the 2σ and 3σ orbitals,

$$2\sigma \approx (0.80)2p_z - (0.47)3d_{z^2} - (0.13)4s,$$
$$3\sigma \approx (0.84)3d_{z^2} + (0.38)2p_z - (0.24)4s$$

TABLE III. Total energies E (E_h), bond distances r_e (Å), dissociation energies D_e (kcal mol^{-1}), harmonic frequencies and anharmonicity corrections ω_e, $\omega_e x_e$ (cm^{-1}), rotational–vibrational coupling constants $\alpha_e \times 10^3$ (cm^{-1}), Mulliken charges on Fe q_{Fe}, and energy separations T_e (cm^{-1}) of the first four states of $^{56}Fe^{16}O^+$.

Method[a]	$-E$	r_e	D_e[b]	ω_e	$\omega_e x_e$	α_e	q_{Fe}	T_e
			$X\,^6\Sigma^+$ (^{6}D)					
MRCI	1337.47567	1.647	72.9	846	6.9	4.3	1.32	0.0
MRCI + Q	1337.50887	1.644	79.9	865	7.3	4.3		0.0
MRCI + DKH2	1346.40968	1.637	72.4	863	7.0	4.4		0.0
MRCI + DKH2 + Q	1346.44316	1.634	79.5	883	7.3	4.3		0.0
C − MRCI	1337.87601	1.644	68.3	856	7.6	4.4		0.0
C − MRCI + Q	1337.95214	1.638	77.3	891	8.4	4.3		0.0
C − MRCI + DKH2	1346.80710	1.635	67.8	872	7.6	4.4		0.0
C − MRCI + DKH2 + Q	1346.88329	1.629	76.9	906	8.0	4.2		0.0
ACPF	1337.50784	1.644	80.2	864	7.5	4.4		0.0
ACPF + DKH2	1346.44224	1.634	79.9	883	7.5	4.4		0.0
C − ACPF	1337.95727	1.639	79.0	888	8.6	4.5		0.0
C − ACPF + DKH2	1346.88860	1.630	78.7	905	8.3	4.3		0.0
RCCSD(T)	1337.51224	1.637	78.5	845	4.5	4.2		0.0
RCCSD(T) + DKH2	1346.44675	1.626	78.2	869	5.3	4.3		0.0
C − RCCSD(T)	1337.97400	1.633	78.5	862	4.9	4.1		0.0
C − RCCSD(T) + DKH2	1346.90516	1.622	78.0	884	5.3	4.2		0.0
MRCI − L	1337.49201	1.645	75.9	801	2.2	4.3		0.0
MRCI − L + Q	1337.51169	1.642	80.3	818	2.8	4.5		0.0
MRCI − L + DKH2	1346.42630	1.631	75.5	838	4.3	4.9		0.0
MRCI − L + DKH2 + Q	1346.44629	1.628	80.0	857	5.0	4.9		0.0
MRCI[c]		1.646	71.2	845				
Expt.		1.643(1)[d]	81.2 ± 0.5[f]	844[e]				
		1.641(1)[e]						
			$a\,^4\Phi$ (^{6}D)					
MRCI	1337.46008	1.672	63.0	690	2.0	4.3	1.31	3421
MRCI + Q	1337.49141	1.662	69.0	706	2.6	4.5		3833
MRCI + DKH2	1346.39256	1.661	61.6	696	2.5	4.6		3756
MRCI + DKH2 + Q	1346.42414	1.648	67.6	714	3.2	4.8		4175
C − MRCI	1337.86295	1.658	60.2	700	2.4	4.9		2867
C − MRCI + Q	1337.93722	1.640	67.7	735	3.9	5.4		3276
C − MRCI + DKH2	1346.79258	1.646	58.9	709	3.3	5.1		3187
C − MRCI + DKH2 + Q	1346.86687	1.632	66.3	747	5.0	5.6		3604
MRCI − L	1337.47375	1.677	64.4	690	2.0	3.7		4007
MRCI − L + Q	1337.49320	1.666	68.7	705	2.8	4.1		4058
MRCI − L + DKH2	1346.40610	1.665	62.9	690	2.2	4.0		4434
MRCI − L + DKH2 + Q	1346.42581	1.653	67.2	707	2.7	4.3		4494
MRCI[c]		1.672	58.7	697				∼ 4300
			$b\,^4\Pi$ (^{6}D)					
MRCI	1337.46007	1.673	63.0	689	1.9	4.2	1.31	3425
MRCI + Q	1337.49135	1.663	68.9	705	2.5	4.5		3846
MRCI + DKH2	1346.39260	1.662	61.6	696	2.5	4.5		3749
MRCI + DKH2 + Q	1346.42415	1.649	67.6	714	3.2	4.8		4173
C − MRCI	1337.86299	1.659	59.8	699	2.3	4.8		2857
C − MRCI + Q	1337.93731	1.641	67.8	733	3.8	5.4		3255
C − MRCI + DKH2	1346.79267	1.646	58.5	708	3.1	5.1		3167
C − MRCI + DKH2 + Q	1346.86704	1.631	66.4	747	4.9	5.6		3566
MRCI − L	1337.47368	1.678	64.4	688	1.9	3.6		4023
MRCI − L + Q	1337.49312	1.667	68.6	704	2.8	4.0		4076
MRCI − L + DKH2	1346.40605	1.666	62.8	690	2.8	4.0		4444
MRCI − L+DKH2 + Q	1346.42578	1.654	67.2	706	2.9	4.4		4501
MRCI[c]		1.684	58.6	696				

TABLE III. (*Continued.*)

Method[a]	$-E$	r_e	D_e[b]	ω_e	$\omega_e x_e$	α_e	q_{Fe}	T_e
			$1\,^4\Delta$ (^{6}D)					
MRCI	1337.45363	1.580	59.0	950($= \Delta G_{1/2}$)			1.37	4838
MRCI + Q	1337.48980	1.578	67.9	951($= \Delta G_{1/2}$)				4186
MRCI + DKH2	1346.38290	1.577	55.6	950($= \Delta G_{1/2}$)				5878
MRCI + DKH2 + Q	1346.41942	1.574	64.6	980($= \Delta G_{1/2}$)				5210
C − MRCI	1337.85531	1.572	55.3	1180($= \Delta G_{1/2}$)				4543
C − MRCI + Q	1337.93512	1.569	66.6	1215($= \Delta G_{1/2}$)				3737
C − MRCI + DKH2	1346.78100	1.567	51.5	1256($= \Delta G_{1/2}$)				5727
C − MRCI + DKH2 + Q	1346.86071	1.564	62.7	1302($= \Delta G_{1/2}$)				4956
MRCI − L	1337.47032	1.581	62.3	966	1.1	3.6		4761
MRCI − L + Q	1337.49155	1.576	67.7	973	0.6	3.6		4420
MRCI − L + DKH2	1346.39975	1.577	58.9	1007($= \Delta G_{1/2}$)				5827
MRCI − L + DKH2 + Q	1346.42124	1.572	64.3	1019($= \Delta G_{1/2}$)				5499
MRCI[c]		1.593	51.0	954				

[a]See Table I for explanation of acronyms and symbols.
[b]With respect to the adiabatic fragments; values in parentheses after the molecular term symbol denote the end term symbol of Fe^+.
[c]Reference 52; MRCI/[6*s*5*p*3*d*1*f*/$_{Fe}$ cc-pVTZ/$_O$] with Stuttgart relativistic small core ($1s^2 2s^2 2p^6$/$_{Fe}$) effective potential.
[d]Reference 49; resonance enhanced photodissociation spectroscopy, r_0 and T_0 values.
[e]Reference 50; microwave spectroscopy, r_0 value.
[f]Reference 30; vacuum UV, D_0 value.

TABLE IV. MRCI + Q total energies E (E_h), bond distances r_e (Å), dissociation energies D_e (kcal mol^{-1}), harmonic frequencies and anharmonicity corrections ω_e, $\omega_e x_e$ (cm^{-1}), rotational–vibrational coupling constants $\alpha_e \times 10^3$ (cm^{-1}), Mulliken charges on Fe q_{Fe}, and energy separations T_e (cm^{-1}) of higher states of $^{56}Fe^{16}O^+$.

State[a]	$-E$	r_e	D_e[b]	ω_e	$\omega_e x_e$	α_e	q_{Fe}	T_e
$1\,^6\Phi$ (^{6}D)	1337.46700	1.792	53.7	818	6.4	2.5	1.38	9189
MRCI[c]		1.807	45.7	712				
$1\,^4\Sigma^+$ (^{6}D)	1337.46567	1.763	52.8	623	2.7	2.6	1.38	9483
MRCI[c]		1.778	44.0	616				
$1\,^6\Pi$ (^{6}D)	1337.46501	1.794	52.4	814	6.5	2.6	1.38	9626
MRCI[c]		1.811	44.7	706				
$2\,^4\Delta$ (^{6}D)	1337.46291	1.747	51.2	926	7.8	–3.4	1.44	10 087
$1\,^4\Sigma^-$ (^{6}D)	1337.45587	1.789	46.7	620	3.3	3.2	1.42	11 633
$2\,^4\Pi$ (^{6}D)	1337.45539	1.749	46.3	587	2.7	2.7	1.37	11 737
MRCI[c]		1.763	39.4	610				
$1\,^2\Pi$ (^{4}F)	1337.44856	1.552	47.8	927($= \Delta G_{1/2}$)			1.11	13 236
$1\,^2\Gamma$ (^{4}F)	1337.44828	1.598	47.7	874	7.8	5.0	1.27	13 298
$1\,^2\Phi$ (^{4}F)	1337.44589	1.629	46.2	810	12.7	6.5	1.14	13 823
$3\,^4\Pi$ (^{6}D)	1337.44442	1.659	39.6	925	7.3	4.5	1.47	14 146
$1\,^2\Sigma^+$ (^{4}F)	1337.44340	1.578	44.7	841	17.1	9.0	1.13	14 370
$2\,^2\Pi$ (^{4}F)	1337.44044	1.632	42.7	982	19.4	3.7	1.19	15 019
$1\,^2\Delta$ (^{4}F)	1337.44024	1.621	42.7	747	7.7	7.0	1.20	15 063
$1\,^2\Sigma^-$ (^{4}F)	1337.43942	1.610	42.2	855	8.0	5.3	1.27	15 243
$2\,^6\Pi$ (^{6}D)	1337.43853	1.835	35.8	711	5.1	3.6	1.32	15 438
MRCI[c]		1.865	31.4	623				
Expt.[d] ($^6\Pi_{7/2}$)		1.900						14 351
$2\,^2\Sigma^+$ (^{4}F)	1337.43557	1.619	39.6	835	5.6	4.3	1.26	16 089
$2\,^2\Delta$ (^{4}F)	1337.43524	1.631	39.5	867	12.9	6.2	1.17	16 161
$2\,^2\Phi$ (^{4}F)	1337.42875	1.607	35.4	865	9.9	5.6	1.14	17 584
$3\,^2\Delta$ (^{4}F)	1337.42477	1.639	33.0	788	13.9	7.7	1.26	18 459
$3\,^2\Pi$ (^{4}F)	1337.41360	1.657	26.2	716	11.5	6.2	1.17	20 909

[a]For MRCI results see supplementary Table S4, Ref. 72.
[b]With respect to adiabatic products; values in parentheses after the molecular term symbol denote the end term symbol of Fe^+.
[c]Reference 52; MRCI/[6*s*5*p*3*d*1*f*/$_{Fe}$ cc-pVTZ/$_O$] with Stuttgart relativistic small core ($1s^2 2s^2 2p^6$/$_{Fe}$) effective potential.
[d]Reference 49; resonance enhanced photodissociation spectroscopy, r_0 and T_0 values.

the emerging bonding can be described by the vbL icon below:

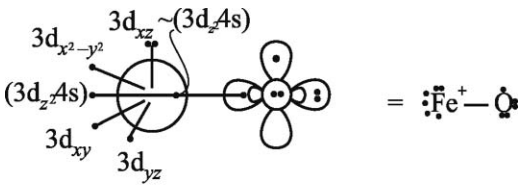

The directly measured ionization energy of FeO ($X\,^5\Delta$) is IE = 8.56 ± 0.01 eV,[30] as compared to the (adiabatic) theoretical C − MRCI + DKH2 + Q (C − ACPF + DKH2) [MRCI − L + DKH2 + Q] {C − RCCSD(T) + DKH2} value, IE = 7.86 (7.99) [8.06] {8.41} eV, with the best agreement obtained at the coupled-cluster level, whereas core + relativistic effects combined contribute less than 0.14 eV depending on the method. The *in situ* positive character of Fe is the cause of the higher IE of FeO relative to that of Fe, (IE = 7.780 eV (Ref. 4)).

2. $a\,^4\Phi$, $b\,^4\Pi$

Located about 4000 cm^{-1} above the $X\,^6\Sigma^+$ the energy difference between the $a\,^4\Phi$ and $b\,^4\Pi$ states is of the order of 10 μE_h and, of course, the "*a*" and "*b*" labeling is only formal. The $a\,^4\Phi$, $b\,^4\Pi$ pair is analogous to the $B\,^5\Pi$, $C\,^5\Phi$ pair of FeO (*vide supra*). Core ($3s^2 3p^6$) + relativistic effects are additive reducing the r_e and D_e values of the $a\,^4\Phi$ ($b\,^4\Pi$) state by 0.022 (0.021) + 0.014(0.014) Å and 1.3 (1.1) + 1.4 (1.3) kcal/mol, whereas core effects alone increase ω_e by 29 (28) cm^{-1}. Thus correcting the MRCI − L + DKH + Q results for core effects, recommended values for both states are r_e = 1.630 Å, D_e = 66.0 kcal/mol, ω_e = 735 cm^{-1}, and T_e = 3900 cm^{-1}. These numbers are very similar to those obtained at the plain MRCI + Q level of theory; see Table III.

The first four MRCI leading equilibrium CFs of the $a\,^4\Phi$ state and corresponding Mulliken distributions are

$$|a^4\Phi\rangle_{B_1} \approx 0.51|1\sigma^2 2\sigma^2 3\sigma^1 1\pi_x^2 1\pi_y^2 2\pi_y^1 1\delta_+^2 1\delta_-^1\rangle - 0.51|1\sigma^2 2\sigma^2 3\sigma^1 1\pi_x^2 1\pi_y^2 2\pi_x^1 1\delta_+^1 1\delta_-^2\rangle + 0.32|1\sigma^2 2\sigma^2 3\sigma^1 1\pi_x^2 \overline{1\pi_y^1} 2\pi_x^1 2\pi_y^1 1\delta_+^1 1\delta_-^2\rangle - 0.32|1\sigma^2 2\sigma^2 3\sigma^1 \overline{1\pi_x^1} 1\pi_y^2 2\pi_x^1 2\pi_y^1 1\delta_+^1 1\delta_-^2\rangle$$

$$4s^{0.31}4p_z^{0.07}4p_x^{0.02}4p_y^{0.02}3d_{z^2}^{1.12}3d_{xz}^{1.06}3d_{yz}^{1.06}3d_{x^2-y^2}^{1.49}3d_{xy}^{1.49} /2s^{1.92}2p_z^{1.54}2p_x^{1.40}2p_y^{1.40}.$$

Leading CFs and populations of the $b\,^4\Pi$ state are identical to those of $a\,^4\Phi$, the only difference being a phase reversal of the second and third configuration. For both states a Fe$^+$–to–O charge transfer of ~0.3 e$^-$ is recorded. The 2σ and 3σ orbitals (identical for both states)

$$2\sigma \approx (0.86)2p_z - (0.36)3d_{z^2} - (0.13)4s,$$

$$3\sigma \approx (0.89)3d_{z^2} - (0.18)4s + (0.29)2p_z$$

along with the populations and the CFs above suggest the following bonding picture:

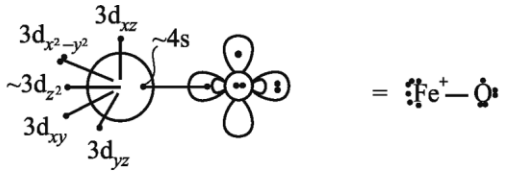

Along the σ-frame nearly 0.4 e$^-$ migrate from Fe$^+$ to the singly occupied $2p_z$ orbital of the O atom, while the 2σ can be considered as the bonding orbital.

3. $1\,^4\Delta$

This is formally the third excited state of FeO$^+$ located ~5000 cm^{-1} above the *X*-state. Using the same analysis as before concerning the relativistic and core effects, our best results at the MRCI − L + DKH2 + Q level corrected for core effects are r_e = 1.572 − 0.009 = 1.563 Å, D_e = 64.3 − 1.3 = 63.0 kcal/mol, and T_e = 5499 − 449 = 5050 cm^{-1} identical to the C − MRCI + DKH2 + Q and similar to the C − MRCI + Q results as in the $a\,^4\Phi$ and $b\,^4\Pi$ states. Overall, ~0.4 e$^-$ are moving from Fe$^+$ to the O atom; see Table III.

The most important MRCI configuration, Mulliken populations, and the 2σ orbital are as follows:

$$|1^4\Delta\rangle \approx 0.80|1\sigma^2 2\sigma^2 1\pi_x^2 1\pi_y^2 2\pi_x^1 2\pi_y^1 1\delta_+^2 1\delta_-^1\rangle$$

$$4s^{0.09}4p_z^{0.05}4p_x^{0.03}4p_y^{0.03}3d_{z^2}^{0.91}3d_{xz}^{1.26}3d_{yz}^{1.26}3d_{x^2-y^2}^{1.97}3d_{xy}^{1.00} /2s^{1.89}2p_z^{1.05}2p_x^{1.67}2p_y^{1.67}$$

$$2\sigma \approx (0.72)2p_z - (0.61)3d_{z^2} + (0.19)2s.$$

The bonding can be described formally as Fe^{2+} (^{5}D; 3d^6) + O$^-$(^{2}P) represented by the vbL diagram below:

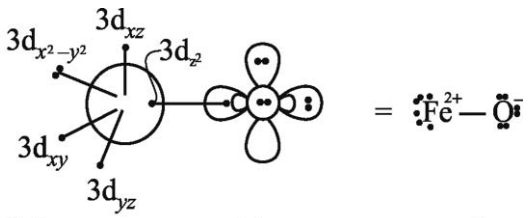

About 0.5 and 0.1 e$^-$ are moving from the O$^-$ to the Fe^{2+} through the π and σ frames, respectively.

4. Higher states

The remaining 20 states listed in Table IV are calculated at the MRCI(+Q)/A5ζ level spanning an energy range of 11 400 cm^{-1}; see Fig. 2. All 20 states are bound with respect to the adiabatic end products as well as to the ground state fragments Fe$^+$ (^{6}D) + O (^{3}P), with MRCI+Q binding energies ranging from 26.2 (3 $^2\Pi$) to about 51–54 (1 $^4\Sigma^+$,

TABLE V. Experimental results from the literature of $^{56}Fe^{16}O^-$. Bond distances r_0 (Å), harmonic frequencies ω_e (cm^{-1}), excitation energies T_e (cm^{-1}), and electron affinities, EA (eV).

State	r_0	ω_e	T_0	EA
X[a]		740 ± 60		1.492 ± 0.020
$X\,^4\Delta_{7/2}$[b]	1.6514 ± 0.0003		0.0	
$X\,^4\Delta_{5/2}$[b]	1.6473 ± 0.0005		226.123(7)	
$X\,^4\Delta_{3/2}$[b]	1.6438 ± 0.0002		465.82(1)	
$A\,^4\Delta_{5/2}$[b]	1.6394 ± 0.0003		12 086.00(8)	
$B^4\Delta_{7/2}$[b]	1.6392 ± 0.0006		12 011.19(5)	
C[b]	1.6604 ± 0.0003		12 225.50(1)	
X[c]				1.50(4)
$X\,^4\Delta_{7/2}$[d]	1.647	740 ± 20		1.495

[a]Reference 11; laser photoelectron spectrometry (PES).
[b]Reference 55; autodetachment spectroscopy. Bond distances calculated from the B values given in Reference 55.
[c]Reference 25; anion PES.
[d]Reference 27; anion ZEKE PES.

$1\,^6\Phi$, $1\,^6\Pi$, $2\,^4\Delta$) kcal/mol. Doublets (12 states) are clustered around a bond distance of 1.60 Å, quartets (5 states) around 1.75 Å, and sextets (3 states) around 1.80 Å, while for all 24 FeO^+ states a charge transfer is observed from Fe^+ to O distinctively less, however, for the doublets. Finally the experimentally assigned state $^6\Pi_{7/2}$ with $T_0 = 14\,351.05$ cm^{-1} and $r_0 = 1.900$ Å (Ref. 49), can be identified to the $2\,^6\Pi$ state of Table IV with $T_e = 15\,438$ cm^{-1} and $r_e = 1.865$ Å in fair agreement with experiment.

MRCI results for higher states of FeO^+ are given in supplementary Table S4. The leading MRCI configurations and atomic populations of the 24 states of FeO^+ are given in supplementary Tables S5 and S6.[72]

C. FeO^-

All experimental results on FeO^- are collected in Table V. According to the experimentalists[27,55,56] there is little doubt that the ground state is $^4\Delta_{7/2}$, with a second $^4\Delta \sim 12\,000$ cm^{-1} higher. As was elaborated in the introduction, however, the recent CASPT2 + DKH calculations of Hendrickx and Anam[37] suggest that the ground state of FeO^- is of $^6\Sigma^+$ symmetry instead of $^4\Delta$. Although it seems that the experimentalists are rather right as to the assignment of the ground state (see also ref 56), it is equally true that the first three states $^6\Sigma^+$, $^4\Delta$, and $^6\Delta$ are very close in energy, rendering a definitive theoretical conclusion as to the symmetry of the ground state problematic (*vide infra*).

The ground state fragments $Fe(^5D;\ 4s^2 3d^6) + O^-(^2P)$ give rise to 18 $^{2S+1}\Lambda$ FeO^- states, 9 quartets and 9 sextets, that is, $^{4,6}(\Phi,\ \Delta[2],\ \Pi[3],\ \Sigma^+[2],\ \Sigma^-)$. We have investigated four states the $X\,^6\Sigma^+$, $a\,^4\Delta$, $A\,^6\Delta$, and $2\,^4\Delta$ *formally* accepting that the ground state is $^6\Sigma^+$ (but see below). Our numerical results at the MRCI − L and RCCSD(T) level are presented in Table VI and PECs are shown in Fig. 3.

Table VI reveals that at the MRCI − L + DKH2 + Q level the ordering of the first three states is $^6\Sigma^+$, $^4\Delta$, $^6\Delta$ with energy separations $T_e = 1636$ and 1830 cm^{-1}, respectively. At the C − RCCSD(T) + DKH2 method, however, these

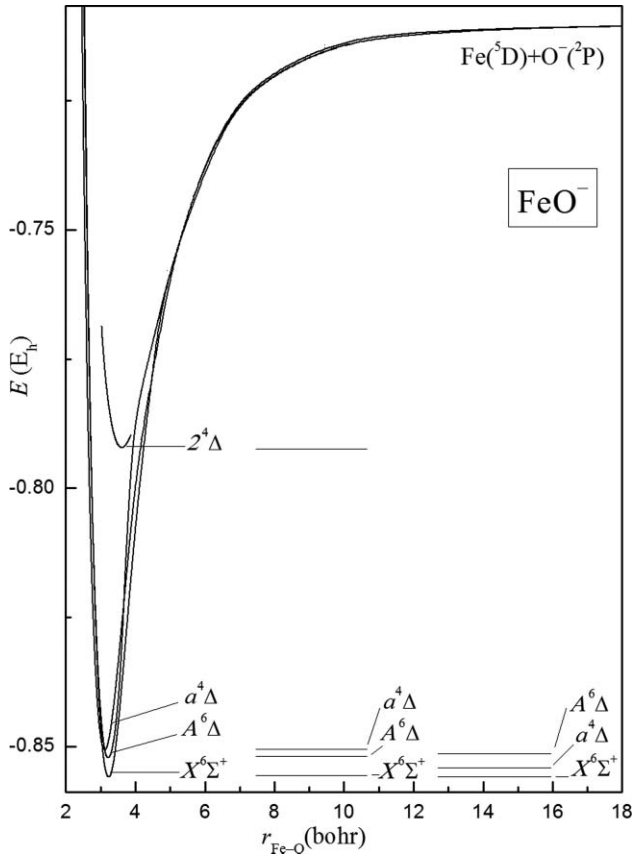

FIG. 3. MRCI − L + Q/A5ζ adiabatic PECs of FeO^-. Left inset at the MRCI − L + Q level. Right inset at the C − RCCSD(T) + DKH2 level.

splittings decrease by more than 1000 cm^{-1} becoming 371 and 917 cm^{-1} mainly due to the core ($3s^2 3p^6$) effects of the metal. Assuming that the coupled-cluster core effects can be "more or less" transferred to the MRCI calculations, it is clear that the $^4\Delta$, and $^6\Delta$ states are practically degenerate to the $^6\Sigma^+$ state. In an effort to investigate the matter further we performed single point calculations for the first three states at the MRCI − L level but without excitation constraints from the CASSCF wavefunction (*vide supra*). The new icMRCI − L′ expansions for the sextets ($^6\Sigma^+$, $^6\Delta$) and the quartet ($^4\Delta$) range from 61×10^6 to 130×10^6 CFs, respectively but at the MRCI − L′ + DKH2 + Q level the sequence and the energy separations remained, in essence, unaltered: $\Delta E(a\,^4\Delta - X\,^6\Sigma^+) = 1479$ and $\Delta E(A\,^6\Delta - X\,^6\Sigma^+) = 1751$ cm^{-1}, as compared to 1636 and 1830 cm^{-1} of the corresponding (truncated) MRCI − L calculations. Correcting those numbers as before for the subvalence $3s^2 3p^6$ electrons of Fe the $a\,^4\Delta - X\,^6\Sigma^+$ and $A\,^6\Delta - X\,^6\Sigma^+$ splittings will certainly decrease significantly, but no more than 1000 cm^{-1}. One more thing has to be accounted for, and this is the spin–orbit coupling of the $a\,^4\Delta$ state. At the MRCI + DKH2/A5ζ level the (diagonal) SO coupling constant A of the $a\,^4\Delta_\Omega$ components is 131 cm^{-1} (*vide infra*), with the $a\,^4\Delta_{7/2}$ component being the lowest, or about 400 cm^{-1}($= 3A$) lower than the $a\,^4\Delta$. This very well means that the $X\,^6\Sigma^+$ state can be found embedded in the $\Omega = \pm 1/2,\ \pm 3/2,\ \pm 5/2,\ \pm 7/2$ manifold of the $^4\Delta_\Omega$ state. The obvious conclusion is that the $X\,^6\Sigma^+$, $a\,^4\Delta$, and $A\,^6\Delta$ states are very close in energy indeed, and for the first

TABLE VI. Total energies E (E_h), bond distances r_e (Å), dissociation energies D_e (kcal mol^{-1}), harmonic frequencies and anharmonicity corrections ω_e, $\omega_e x_e$ (cm^{-1}), rotational–vibrational coupling constants $\alpha_e \times 10^3$ (cm^{-1}), Mulliken charges Fe q_{Fe}, and energy separations T_e (cm^{-1}) of $^{56}Fe^{16}O^-$.

Method[a]	$-E$	r_e	D_e[b]	ω_e	$\omega_e x_e$	α_e	q_{Fe}	T_e
			$X\,^6\Sigma^+$					
MRCI − L	1337.81834	1.709	90.4	819	3.8	2.7	−0.33	0.0
MRCI − L + Q	1337.85634	1.710	91.5	832	2.9	2.1		0.0
MRCI − L + DKH2	1346.75764	1.699	91.5	758	−4.8	2.2		0.0
MRCI − L + DKH2 + Q	1346.79584	1.709	92.4	752	−7.2	1.4		0.0
RCCSD(T)	1337.86928	1.691	92.3	893	3.0	2.0		0.0
RCCSD(T) + DKH2	1346.80997	1.690	93.9	857	−2.1	1.5		0.0
C − RCCSD(T)	1338.33067	1.686	90.3	898	3.2	2.2		0.0
C − RCCSD(T) + DKH2	1347.26843	1.685	91.9	878	−0.1	1.9		0.0
CASPT2[c]		1.683		807				
			$a\,^4\Delta$					
MRCI − L	1337.81312	1.649	87.1	831	7.2	4.4	−0.44	1147
MRCI − L + Q	1337.85110	1.648	88.2	849	6.5	4.0		1151
MRCI − L + DKH2	1346.74992	1.643	86.7	839	7.3	4.4		1695
MRCI − L +DK H2 + Q	1346.78839	1.642	87.8	855	6.5	4.1		1636
RCCSD(T)	1337.86632	1.638	90.5	870	5.6	4.1		649
RCCSD(T) + DKH2	1346.80374	1.631	90.0	882	5.8	4.1		1369
C − RCCSD(T)	1338.33287	1.626	91.6	882	5.7	4.1		−483
C − RCCSD(T) + DKH2	1347.26674	1.619	90.8	896	5.7	4.1		371
CASPT2[c]		1.634		878				1049
Expt.[d]		1.647		740 ± 20				
			$A\,^6\Delta$					
MRCI − L	1337.81091	1.699	85.7	822	2.9	3.6	−0.01	1631
MRCI − L + Q	1337.85252	1.695	89.1	827	1.7	2.2		838
MRCI − L + DKH2	1346.74563	1.694	83.9	819	2.8	4.9		2636
MRCI − L + DKH2 + Q	1346.78750	1.690	87.2	817	4.6	4.4		1830
RCCSD(T)	1337.86671	1.713	90.7	768	3.6	2.8		564
RCCSD(T) + DKH2	1346.80188	1.708	88.9	769	3.5	2.9		1776
C − RCCSD(T)	1338.33259	1.703	91.5	780	3.2	2.9		−422
C − RCCSD(T) + DKH2	1347.26426	1.699	89.3	780	3.0	3.0		917
CASPT2[c]		1.688		830				2904
			$2\,^4\Delta$					
MRCI − L	1337.75764	1.926	52.3	440	3.9	3.1	−0.49	13 321
MRCI − L + Q	1337.79225	1.908	51.3	437	3.9	2.9		14 066
MRCI − L + DKH2	1346.69362	1.916	51.3	434	3.5	3.1		14 051
MRCI − L + DKH2 + Q	1346.72876	1.896	50.4	431	3.5	2.9		14 722
Expt.[e]		1.6392						∼12 000

[a]See Table I for explanation of acronyms and symbols.
[b]With respect to the adiabatic fragments, Fe(^{5}D) + O$^-$(^{2}P).
[c]Reference 37
[d]Reference 27; anion ZEKE PES.
[e]Reference 55

two states the "X" and "a" labeling is formal according to our calculations. This "conflict" between experiment ($X\,^4\Delta$) (Refs. 55 and 27) and theory ($X\,^6\Sigma^+$) is quite interesting and productive, indicating once more the inherent difficulties of obtaining reliable *ab initio* all electron results even for systems as simple chemically, but not computationally, as the FeO^- anion. Observe that the MRCI − L + DKH2 + Q bond distance of the $a\,^4\Delta$ state (but $X\,^4\Delta$ for the experimentalists), is $r_e = 1.642$ Å in respectable agreement with the experimental value of $r_0 = 1.647$ Å,[27] but we cannot say the same for the ω_e value: ω_e(theory) − ω_e(experiment) ≈100 cm^{-1}; see Table VI.

For the $2\,^4\Delta$ state located experimentally ∼12 000 cm^{-1} above the X-state, with respect to the $a\,^4\Delta$ state, our MRCI − L + DKH2 + Q value is 14 722 − 1636 + $\Delta\omega_e/2$ = 12 874 cm^{-1} in good agreement with experiment; however, the corresponding r_e is calculated to be 0.25 Å larger than the experimental one;[55] see Table V.

The dissociation energy of the FeO^- ($X\,^6\Sigma^+$) practically the same to the $a\,^4\Delta$, is D_e = 92.4 (91.9) kcal/mol or D_0 = 91.3 (90.6) kcal/mol at the MRCI − L + DKH2 + Q (C − RCCSD(T) + DKH2) level of theory, about 6 kcal/mol less than the experimental value of 97.2 kcal/mol. The latter has been derived from the energy conservation relation $D_0(FeO^-)$ = D_0(FeO) + EA(FeO) − EA(O) = 96.4 (Ref. 29) + 34.48 (Ref. 27) − 33.69 (Ref. 71) = 97.2 kcal/mol. The calculated [experimental] MRCI − L + DKH2 + Q (C − RCCSD(T) + DKH2) electron affinity of FeO is EA = 1.454 (1.466) [1.495 (Ref. 27)] eV, the combined core + DKH2 effects contributing + 0.03 eV at the coupled-cluster level.

We turn now to the bonding nature of FeO^-. For the $X\,^6\Sigma^+$, $a\,^4\Delta$, $A\,^6\Delta$, $2\,^4\Delta$ states the total O^-–to–Fe Mulliken charge transfer is around 0.3, 0.4, 0.0, and 0.5 e^-, respectively. The leading MRCI configurations of $X\,^6\Sigma^+$ and $a\,^4\Delta$ are

$$|X^6\Sigma^+\rangle \approx 0.82|1\sigma^2 2\sigma^2 3\sigma^2 4\sigma^1 1\pi_x^2 1\pi_y^2 2\pi_x^1 2\pi_y^1 1\delta_+^1 1\delta_-^1\rangle$$

$$|a^4\Delta\rangle_{A_1} \approx 0.86|1\sigma^2 2\sigma^2 3\sigma^2 1\pi_x^2 1\pi_y^2 2\pi_x^1 2\pi_y^1 1\delta_+^2 1\delta_-^1\rangle$$

identical to the main configurations of $A\,^5\Sigma^+$ and $X\,^5\Delta$ of the neutral FeO after attaching one electron to the σ frames, $4\sigma^1(X\,^6\Sigma^+)$ and $3\sigma^1(X\,^5\Delta) \rightarrow 3\sigma^2(a\,^4\Delta)$. The atomic populations as well of the two states above are very similar to the populations of the $A\,^5\Sigma^+$ and $X\,^5\Delta$ states of FeO after adding about one electron to their 4*s* atomic distributions. Therefore, the bonding in FeO^- can be described by the vbL diagrams of the $A\,^5\Sigma^+$ and $X\,^5\Delta$ states of FeO, the extra electron attached to the *in situ* Fe^+ ($X\,^5\Delta \rightarrow a\,^4\Delta$) and to a $4\sigma^1$ ($A\,^5\Sigma^+ \rightarrow X\,^6\Sigma^+$) orbital creating a "two center-three electron" bond for the $X\,^6\Sigma^+$ state. Recall that within the accuracy of our calculations the $X\,^5\Delta$ and $A\,^5\Sigma^+$ states of FeO are degenerate (*vide supra*), and this degeneracy is reflected to the analogous $X\,^6\Sigma^+$ and $a\,^4\Delta$ states of FeO^-.

The leading MRCI configurations and corresponding populations for the four states of FeO^- are given in supplementary Tables S7 and S8.[72]

IV. SPIN–ORBIT COUPLING CONSTANTS

For the first three non-Σ low-lying states of FeO and FeO^+ and the first two of FeO^-, we report below diagonal spin–orbit coupling constants *A* (cm^{-1}) at the MRCI + DKH2/A5ζ level; experimental values in parenthesis.

FeO	*A*	FeO^+	*A*	FeO^-	*A*
$X\,^5\Delta$	102 (97) (Ref. 27)	$a\,^4\Phi$	62	$a\,^4\Delta$	131 (120) (Ref. 55)
$A\,^5\Pi$	236	$b\,^4\Pi$	169	$A\,^6\Delta$	83
$B\,^5\Phi$	79	$1\,^4\Delta$	127		

V. SYNOPSIS AND FINAL REMARKS

We believe that this is the first systematic high level *ab initio* all electron study of the iron monoxide species FeO, FeO^+, and FeO^- employing correlation consistent basis sets of quintuple quality and a variety of highly correlated methods. At the MRCI + Q/A5ζ level we have constructed for the first time full PECs for 48, 24, and 4 bound states of FeO, FeO^+, and FeO^-, respectively. For a few low-lying states of FeO and FeO^+ subvalence ($3s^2 3p^6$) and scalar relativistic effects through the DKH2 approximation have been taken into account; no core effects were included in the calculations of FeO^- due to the resulting unmanageable large C − MRCI − L expansions. We report energetics, common spectroscopic parameters (r_e, ω_e, $\omega_e x_e$, α_e), dipole moments, and spin–orbit coupling constants *A*. Although overall our results are in good agreement with experiment, there are still serious discrepancies between theory and experiment, assuming always of course that the experimental numbers are correct. For example our calculations predict that the $X\,^5\Delta$ and $A\,^5\Sigma^+$ states of FeO are quasi-degenerate, contrary to the experimental $A\,^5\Sigma^+ - X\,^5\Delta$ separation of ~0.5 eV. In addition, we are off by ~10% in the dissociation energy of the FeO($X\,^5\Delta$), whereas the calculated dipole moment for the same state seems to converge to ~0.8 D higher than the experimental one. For the FeO^- the calculated ground state is *formally* $X\,^6\Sigma^+$ as contrasted to the $X\,^4\Delta$ of the experiment, but independently of their ordering these two states are practically degenerate, thus very difficult to be "reliably" resolved computationally. It should be observed on the other hand that while three FeO^- states are crowded within ~1000 cm^{-1} ($X\,^6\Sigma^+$, $a\,^4\Delta$, $A\,^6\Delta$), the experimentalists have recorded only one ($X\,^4\Delta$).

In all states of FeO a Fe–to–O charge transfer is observed ranging from 0.5 to 0.7 e^-; therefore, the bonding in FeO can better be understood as Fe^+ in the field of O^-. Even in FeO^+ a Fe^+–to–O charge transfer of ~ 0.3 e^- is observed for most of the states.

We can claim that, overall, and taking into consideration the large basis sets and the variety of methods used, our conclusions are in general trustworthy. This, in combination with the plethora of states examined along with the construction of full PECs, we believe to be quite informative and valuable to all who are interested in the 3*d*-metal oxides and in particular on the FeO, FeO^+, and FeO^- species.

ACKNOWLEDGMENTS

One of us (C.N.S.) would like to express his gratitude to the Special Funding Research Account (EΛKE) of the National and Kapodistrian University of Athens for financial support.

[1] E. Miliordos and A. Mavridis, J. Phys. Chem. A **111**, 1953 (2007).
[2] E. Miliordos and A. Mavridis, J. Phys. Chem. A **114**, 8536 (2010).
[3] J. F. Harrison, Chem. Rev. **100**, 679 (2000), and references therein.
[4] Y. Ralchenko, A. E. Kramida, J. Reader, and NIST ASD Team (2010). NIST Atomic Spectra Database (version 4.0) (National Institute of Standards and Technology, Gaithersburg, MD), online available at: http://physics.nist.gov/asd [accessed December 17, 2010].
[5] B. Rosen, Nature (London) **156**, 570 (1945).
[6] R. F. Barrow and M. Senior, Nature (London) **223**, 1359 (1969).
[7] G. Balducci, G. De Maria, M. Guido, and V. Piacente, J. Chem. Phys. **55**, 2596 (1971).
[8] D. E. Jensen and G. A. Jones, J. Chem. Soc., Faraday Trans. 1 **69**, 1448 (1973).
[9] J. B. West and H. P. Broida, J. Chem. Phys. **62**, 2566 (1975).
[10] D. L. Hildenbrand, Chem. Phys. Lett. **34**, 352 (1975).
[11] P. C. Engelking and W. C. Lineberger, J. Chem. Phys. **66**, 5054 (1977).
[12] T. C. DeVore and T. N. Gallaher, J. Chem. Phys. **70**, 4429 (1979).
[13] D. W. Green and G. T. Reedy, J. Mol. Spectrosc. **78**, 257 (1979).
[14] S. M. Harris and R. F. Barrow, J. Mol. Spectrosc. **84**, 334 (1980).
[15] E. Murad, J. Chem. Phys. **73**, 1381 (1980).
[16] A. S.-C. Cheung, R. M. Gordon, and A. J. Merer, J. Mol. Spectrosc. **87**, 289 (1981).
[17] A. S.-C. Cheung, N. Lee, A. M. Lyyra, A. J. Merer, and A. W. Taylor, J. Mol. Spectrosc. **95**, 213 (1982).
[18] S. Smoes and J. Drowart, High Temp. Sci. **17**, 31 (1984).
[19] A. W. Taylor, A. S.-C. Cheung, and A. J. Merer, J. Mol. Spectrosc. **113**, 487 (1985).
[20] T. Kröckertskothen, H. Knöckel, and E. Tiemann, Mol. Phys. **62**, 1031 (1987).
[21] T. C. Steimle, D. F. Nachman, J. E. Shirley, and A. J. Merer, J. Chem. Phys. **90**, 5360 (1989).
[22] A. J. Merer, Annu. Rev. Phys. Chem. **40**, 407 (1989).
[23] J. Fan and L.-S. Wang, J. Chem. Phys. **102**, 8714 (1995).

[24]M. Barnes, M. M. Fraser, P. G. Hajigeorgiou, A. J. Merer, and S. D. Rosner, J. Mol. Spectrosc. **170**, 449 (1995).
[25]H. Wu, S. R. Desai, and L.-S. Wang, J. Am. Chem. Soc. **118**, 5296 (1996); *ibid.* **118**, 7434 (1996).
[26]M. D. Allen, L. M. Ziurys, and J. M. Brown, Chem. Phys. Lett. **257**, 130 (1996).
[27]G. Drechsler, U. Boesl, C. Bäßmann, and E. W. Schlag, J. Chem. Phys. **107**, 2284 (1997).
[28]T. C. Steimle, J. Gengler, and P. J. Hodges, J. Chem. Phys. **121**, 12303 (2004).
[29]D. A. Chestakov, D. H. Parker, and A. V. Baklanov, J. Chem. Phys. **122**, 084302 (2005).
[30]R. B. Metz, C. Nicolas, M. Ahmed, and S. R. Leone, J. Chem. Phys. **123**, 114313 (2005).
[31]P. S. Bagus and H. J. T. Preston, J. Chem. Phys. **59**, 2986 (1973).
[32]M. Krauss and W. J. Stevens, J. Chem. Phys. **82**, 5584 (1985).
[33]M. Dolg, U. Wedig, H. Stoll, and H. Preuss, J. Chem. Phys. **86**, 2123 (1987).
[34]C. W. Bauschlicher, Jr., S. R. Langhoff, and A. Komornicki, Theor. Chim. Acta **77**, 263 (1990).
[35]C. W. Bauschlicher, Jr. and P. Maitre, Theor. Chim. Acta **90**, 189 (1995).
[36]W. Cardoen and R. J. Gdanitz, Chem. Phys. Lett. **364**, 39 (2002).
[37]M. F. A. Hendrickx and K. R. Anam, J. Phys. Chem. A **113**, 8746 (2009).
[38]D. Tzeli and A. Mavridis, J. Chem. Phys. **118**, 4984 (2003); *ibid.* **132**, 194312 (2010).
[39]G. V. Chertihin, W. Saffel, J. T. Yustein, L. Andrews, M. Neurock, A. Ricca, and C. W. Bauschlicher, Jr., J. Phys. Chem. **100**, 5261 (1996).
[40]G. L. Gutsev, S. N. Khanna, B. K. Rao, and P. Jena, J. Phys. Chem. A **103**, 5812 (1999).
[41]A. J. Bridgeman and J. Rothery, J. Chem. Soc., Dalton Trans. 211 (2000).
[42]G. L. Gutsev, B. K. Rao, and P. Jena, J. Phys. Chem. A **104**, 5374 (2000).
[43]E. L. Uzunova, H. Mikosch, and G. S. Nikolov, J. Chem. Phys. **128**, 094307 (2008).
[44]P. B. Armentrout, L. F. Halle, and J. L. Beauchamp, J. Chem. Phys. **76**, 2449 (1982).
[45]R. L. Hettich, T. C. Jackson, E. M. Stanko, and B. S. Freiser, J. Am. Chem. Soc. **108**, 5086 (1986).
[46]S. K. Loh, E. R. Fisher, L. Lian, R. H. Schultz, and P. B. Armentrout, J. Phys. Chem. **93**, 3159 (1989).
[47]J. B. Griffin and P. B. Armentrout, J. Chem. Phys. **107**, 5345 (1997).
[48]J. Husband, F. Aguirre, P. Ferguson, and R. B. Metz, J. Chem. Phys. **111**, 1433 (1999).
[49]F. Aguirre, J. Husband, C. J. Thompson, K. L. Stringer, and R. B. Metz, J. Chem. Phys. **119**, 10194 (2003).
[50]D. T. Halfen and L. M. Ziurys, Chem. Phys. Lett. **496**, 8 (2010).
[51]A. Fiedler, J. Hrušák, W. Koch, and H. Schwarz, Chem. Phys. Lett. **211**, 242 (1993).
[52]Y. Nakao, K. Hirao, and T. Taketsugu, J. Chem. Phys. **114**, 7935 (2001).
[53]A. Fiedler, D. Schröder, S. Shaik, and H. Schwarz, J. Am. Chem. Soc. **116**, 10734 (1994).
[54]K. Hirao, Chem. Phys. Lett. **190**, 374 (1992); *ibid.* **196**, 397 (1992); *ibid.* **201**, 59 (1993).
[55]T. Andersen, K. R. Lykke, D. M. Neumark, and W. C. Lineberger, J. Chem. Phys. **86**, 1858 (1987).
[56]D. M. Neumark and W. C. Lineberger, J. Phys. Chem. A **113**, 10588 (2009).
[57]T. H. Dunning, Jr., J. Chem. Phys. **90**, 1007 (1989).
[58]N. B. Balabanov and K. A. Peterson, J. Chem. Phys. **123**, 064107 (2005).
[59]R. A. Kendall, T. H. Dunning, Jr., and R. J. Harrison, J. Chem. Phys. **96**, 6796 (1992).
[60]K. Raghavachari, G. W. Trucks, J. A. Pople, and M. Head-Gordon, Chem. Phys. Lett. **157**, 479 (1989); J. D. Watts and R. J. Bartlett, J. Chem. Phys. **98**, 8718 (1993); P. J. Knowles, C. Hampel, and H.-J. Werner, *ibid.* **99**, 5219 (1993); *ibid.* **112**, 3106E (2000).
[61]H.-J. Werner and P. J. Knowles, J. Chem. Phys. **89**, 5803 (1988); P. J. Knowles and H.-J. Werner, Chem. Phys. Lett. **145**, 514 (1988).
[62]M. Douglas and N. M. Kroll, Ann. Phys. **82**, 89 (1974).
[63]B. A. Hess, Phys. Rev. A: At. Mol. Opt. Phys. **32**, 756 (1985); *ibid.* **33**, 3742 (1986).
[64]H. B. Jansen and P. Ross, Chem. Phys. Lett. **3**, 140 (1969); S. F. Boys and F. Bernardi, Mol. Phys. **19**, 553 (1970).
[65]S. R. Langhoff and E. R. Davidson, Int. J. Quantum Chem. **8**, 61 (1974); E. R. Davidson and D. W. Silver, Chem. Phys. Lett. **52**, 403 (1977).
[66]R. J. Gdanitz and R. Ahlrichs, Chem. Phys. Lett. **143**, 413 (1988); H.-J. Werner and P. J. Knowles, Theor. Chim. Acta **78**, 175 (1990).
[67]MOLPRO, a package of *ab initio* programs designed by H.-J. Werner and P. J. Knowles, version 2006.1, R. Lindh, F. R. Manby, M. Schütz, *et al.*.
[68]C. E. Bunge, J. A. Barrientos, and A. V. Bunge, At. Data Nucl. Data Tables **53**, 113 (1993).
[69]T. Helgaker, W. Klopper, H. Koch, and J. Noga, J. Chem. Phys. **106**, 9639 (1997).
[70]C. Puzzarini, Int. J. Quantum Chem. **110**, 2483 (2010).
[71]O. Blondel, W. Chaibi, C. Delsart, C. Drag, F. Goldfarb, and S. Kröger, Eur. Phys. J. D **33**, 335 (2005).
[72]See supplementary material at http://dx.doi.org/10.1063/1.3598529 for MRCI results for higher states of FeO and FeO^+ as well as leading MRCI/A5ζ configurations, Mulliken atomic populations, and atomic charges of 45, 24, and 4 states of FeO, FeO^+, and FeO^- respectively.